DANMARKS OG GRØNLANDS GEOLOGISKE UNDERSØGELSE **RAPPORT 2023/11**

Compositional characterisation of Nini dead oil and remaining oil in preserved, cleaned, restored, and CO_2-flooded core plugs from the Nini-4 well, Nini West reservoir

Project Greensand Phase 2, WP 3.3

Henrik I. Petersen, Wael Fadi Al-Masri, Arka Rudra,
Samira Mohammadkhani & Hamed Sanei

GEOLOGICAL SURVEY OF DENMARK AND GREENLAND
DANISH MINISTRY OF CLIMATE, ENERGY AND UTILITIES

G E U S

Compositional characterisation of Nini dead oil and remaining oil in preserved, cleaned, restored, and CO_2-flooded core plugs from the Nini-4 well, Nini West reservoir

Project Greensand Phase 2, WP 3.3,

Henrik I. Petersen, Wael Fadi Al-Masri, Arka Rudra,
Samira Mohammadkhani & Hamed Sanei

Confidential report

Copy No.

Released 31.12.2023

GEOLOGICAL SURVEY OF DENMARK AND GREENLAND
DANISH MINISTRY OF CLIMATE, ENERGY AND UTILITIES

G E U S

EUDP

Det Energiteknologiske Udviklings- og Demonstrationsprogram

Funded by the European Union
NextGenerationEU

GREEN SAND

Project Greensand Phase 2

WP 3.3:

Compositional characterisation of Nini dead oil and remaining oil in preserved, cleaned, restored, and CO_2-flooded core plugs from the Nini-4 well, Nini West reservoir

COMPOSITIONAL CHARACTERISATION OF NINI DEAD OIL AND REMAINING OIL IN PRESERVED, CLEANED, RESTORED, AND CO_2-FLOODED CORE PLUGS FROM THE NINI-4 WELL, NINI WEST RESERVOIR

Project Greensand Phase 2, WP3.3

Confidential GEUS Report. Released 31/12 2023

AUTHORS: HENRIK I. PETERSEN, WAEL FADI AL-MASRI, ARKA RUDRA, SAMIRA MOHAMMADKHANI, HAMED SANEI

CONTENTS

SUMMARY

The depleted Nini West oilfield (Siri Canyon, Danish North Sea) is considered a potential storage site for the safe sequestration of CO_2 in the Paleogene quartz- and glauconite-rich reservoir sandstones. The current study focuses on injectivity risks associated with reactions between injected CO_2 and the unproduced, remaining oil present in the depleted reservoir of the field. The main process investigated is the scenario in which the injected supercritical (sc) CO_2 dissolves certain fractions of the remaining oil, while other fractions, such as solid bitumen/asphaltenes, may be immobile and may have an adverse effect on reservoir capacity and CO_2 injectivity by clogging critical pore throats of the pore network.

The current study investigates the composition of the Nini stock tank oil (STO), preserved core extracts, and the remaining oil in core plugs from the reservoir sandstone. A total of 13 core plugs from the Nini-4 well oil leg were analysed, including three 'fresh' preserved plugs, three preserved plugs stored in brine, five plugs cleaned by three different methods, one restored plug, and one restored $scCO_2$-flooded plug. The hydrocarbon composition of the STO and the core extracts was characterised by gas chromatography and organic petrography. The oil in the core plugs was analysed by organic petrography and extended slow heating pyrolysis (ESH®) providing a detailed insight into the occurrence and distribution of the oil and solid bitumen/asphaltene fractions in the various plugs.

Minor oil-based mud (OBM) contamination in the diesel range was recorded in the STO and core extracts indicating that it will not interfere with the heavy oil fraction $>nC_{20}$ which may pose problems with clogging. The STO contains only a minor amount of asphaltenes. The remaining oil in the preserved plugs consists mainly of mobile oil and a lesser amount of immobile oil and solid bitumen/asphaltenes. All three cleaning methods remove most oil fractions, but none of them, including the hot Soxhlet extraction method, can remove all the solid bitumen/asphaltenes associated with glauconite. These solid bitumen/asphaltenes occur in the interior of glauconite clasts, as coatings on the surface, and in small cracks in the surface, as well as between the laminae of glauconised mica. The remaining solid bitumen/asphaltenes are 'carried' over to the restored (STO saturated and aged) plugs used for $scCO_2$-flooding experiments. A hot Soxhlet extraction cleaned plug was restored by saturation with synthetic formation brine, drainage to initial water saturation, and at the end saturation with STO and ageing for one month. The oil occurs as surface coatings and in the interior of glauconite clasts, between the laminae of glauconised mica, and as a hydrocarbon ooze. The restored oil composition is, overall, comparable to the composition of the oil in the preserved plugs.

Supercritical CO_2-flooding of a restored plug shows that the mobile oil fractions are removed while the solid bitumen/asphaltenes coatings and remnants in the interior of the glauconite clasts were not mobilised. This suggests that the solid bitumen/asphaltenes are non-movable, and that the glauconite clasts associated with solid bitumen/asphaltenes can be considered to have oil-wet surfaces. The solid bitumen/asphaltenes may have a protective effect thus mitigating glauconite swelling, disintegration, and fines generation. Glauconite clasts not associated with solid bitumen/asphaltenes are likely water-wet and potentially prone to both swelling and disintegration into fines. Negligible amounts of immobile oil are left behind in the $scCO_2$-flooded core plug, and the saturation of solid bitumen/asphaltenes is very similar to those of the cleaned core plugs which together with the inferior immobile oil fraction indicate no or very low risk for precipitation of solid bitumen/asphaltenes.

Measured He-porosity is slightly underestimated due to the presence of non-movable solid bitumen/asphaltenes in the cleaned plugs. A method to convert the results of vol.%-ESH to %-saturation has been derived, and the equation required to correct the He-porosimeter porosity measurements by a correction factor has been developed based on the results of the ESH from cleaned core plugs. The porosity underestimation ranges from 0.432–1.138 PU. The calculated total oil saturation from ESH data of a restored plug provides almost the exact measured saturation value, and the determined non-movable oil saturations of preserved and restored core plugs are within the range of measured residual oil saturations. This indicates that the ESH method might be used to provide a fast and low-cost estimate of the residual oil saturation after water flooding. This assumption should be verified by ESH analysis of water flooded samples.

INTRODUCTION

The EUDP-funded "Project Greensand Phase 2" aims at storing CO_2 in the Nini West Field in the Siri Canyon in the Danish North Sea by injecting supercritical CO_2 ($scCO_2$) into the Palaeocene-Eocene reservoir sandstones. Nini West is a depleted oil field and is considered a potential storage site for the safe sequestration of CO_2 as an integrated part of Denmark's ambition to reduce CO_2 emissions using carbon capture storage (CCS) technologies. It has been demonstrated that the Nini West field is conceptually suitable for injecting 0.45 million tonnes of CO_2 per year per well for 10 years and that the storage site can contain a vertical column of $scCO_2$ of a minimum of ~600 m, providing a comfortable seal safety column-overhead (Petersen et al., 2022).

This report presents the results of work package 3.3 (WP3.3), "Effects of residual oil on the rock matrix and injectivity". $scCO_2$ is a strong solvent of hydrocarbon residues and may potentially mobilise these in the reservoir, causing higher oil displacement and leakage or clogging of pore throats (Hwang & Ortiz, 1998; Jarboe et al., 2015). These potential risks were identified but not addressed in Greensand Phase 1. The movable part of the remaining oil and immobility of the heavier fractions, such as solid bitumen/asphaltenes, may pose a potential risk by having an adverse effect on reservoir storage capacity and CO_2 injectivity. The injected $scCO_2$ may dissolve certain fractions of the remaining oil and produce a miscible CO_2-oil phase, which is mobilised. During the migration of this miscible CO_2-oil phase, solid bitumen/asphaltenes may precipitate, particularly when the injection pressure drops. This precipitation may lead to the accumulation of immobile solid bitumen/asphaltenes at the critical orifices of the pore networks and, together with solid bitumen/asphaltenes already present in the reservoir, potentially lead to early clogging of pore throats near the injection well (Hwang & Ortiz, 1998).

Laboratory scale $scCO_2$-flooding experiments are commonly conducted to investigate and de-risk potential risk elements during $scCO_2$ injection, including the effect of remaining oil on injectivity and aspects such as rock matrix alterations. This study investigates the remaining oil in the rock matrix of the Nini West reservoir sandstones by analysing the hydrocarbon composition of the Nini dead oil (stock tank oil, STO) and core extracts and quantifying the amounts of mobile and immobile oil and solid bitumen/asphaltenes in preserved, cleaned, restored and $scCO_2$-flooded core plugs. The hydrocarbon composition of the dead oil and the core extracts will be characterised by 'conventional' organic geochemistry (bulk composition and gas chromatography). In contrast, the remaining oil in the various core plugs will be characterised by a unique pyrolysis technique and organic petrography to provide a detailed insight into the occurrence and distribution of the mobile and immobile oil fractions in the reservoir.

The analyses will, in combination, address several important aspects of the remaining oil in the reservoir and core plugs used for $scCO_2$-flooding experiments with the presence of oil:

1. Geochemical characterisation of the STO and core extracts from preserved cores. This will provide general compositional information on the produced oil and the extractable oil fraction, together with a detailed determination of the mobile and immobile oil fractions in the preserved cores.

2. Quantification of the fractions of mobile and immobile oil and solid bitumen/asphaltenes in plugs cleaned by different methods. In combination with organic petrography, this will evaluate the efficiency of different cleaning methods to remove the remaining oil from core plugs to be restored for $scCO_2$-flooding experiments.

3. Quantification and organic petrography of the mobile oil, immobile oil, and solid bitumen/asphaltene fractions in a cleaned core plug restored to initial water and residual oil saturations for a $scCO_2$-flooding experiment with the presence of oil (CO_2-brine-oil). The restoration

is a complex procedure in which stock tank oil is used to saturate the core plug, followed by a one month ageing period. Laboratory scale $scCO_2$-flooding experiments investigate and de-risk potential risk elements during $scCO_2$ injection, including remaining oil's effect on injectivity and aspects such as rock matrix alterations.

4. Quantification and organic petrography of the mobile oil, immobile oil, and solid bitumen/asphaltene fractions in a restored plug (point 3) after $scCO_2$ flooding. This will demonstrate the effect of $scCO_2$ flooding on the remaining oil composition.

The outcome of the analyses will increase the understanding of the composition of the remaining oil and the effect of $scCO_2$ injection on the oil composition, particularly regarding the mobile and immobile oil, and solid bitumen/asphaltene fractions. The results are expected to be used to de-risk clogging issues related to the solid bitumen/asphaltenes.

GEOLOGICAL SETTING

The Palaeocene Siri Canyon extends about 120 km E–NE from the Danish Central Graben eastern boundary across the Ringkøbing-Fyn High towards the Stavanger Platform (Figure 1). It is formed by erosion into the underlying Cretaceous–Danian Chalk Group. A turbidite system transported glauconite-rich sand from the Stavanger Platform through the canyon to the Danish Central Graben. During the Palaeocene–Miocene, the canyon was filled with hemipelagic and turbiditic marls and mudstones, while Palaeocene–Eocene sandy mass flows and turbidites deposited well-sorted, fine-grained glauconitic sandstones (Hamberg et al., 2005; Schiøler et al., 2007; Weibel et al., 2010). Sandstone deposition occurred as a response to Palaeogene backstepping of the turbidite system. The sandstones are encased in deep-water pelagic mudstones of the Rogaland Group (Våle to Balder Formations; Figure 2) (Hamberg et al., 2005; Schiøler et al., 2007; Nielsen et al., 2015). The sandstone reservoir geometry can be rather complex due to remobilisation caused by post-depositional fluidisation (Hamberg et al., 2005; Svendsen et al., 2010). The sandstones can therefore occur at different levels in the stratigraphy, with the oldest sealed by formations within the Rogaland Group and the youngest by the overlying regionally distributed Eocene Horda and Oligocene–Miocene Lark Formations (Figure 2). The Bor, Tyr, Idun, Rind and Kolga sandstones can all be hydrocarbon-bearing reservoirs in the Siri Canyon. However, in Nini West, the reservoir is constituted by the Kolga sandstones that have been remobilised into the Balder Formation (Svendsen et al., 2020).

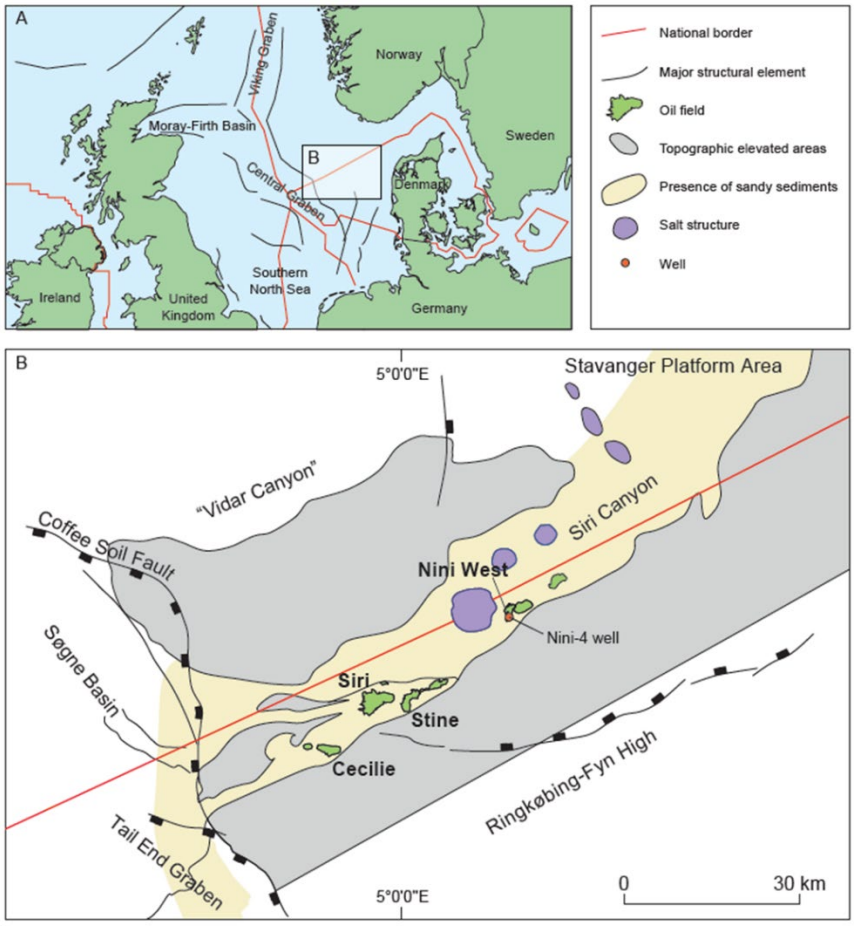

Figure 1. The Nini West oil field location in the Siri Canyon east of the Danish Central Graben, North Sea. Modified from Petersen et al. (2022).

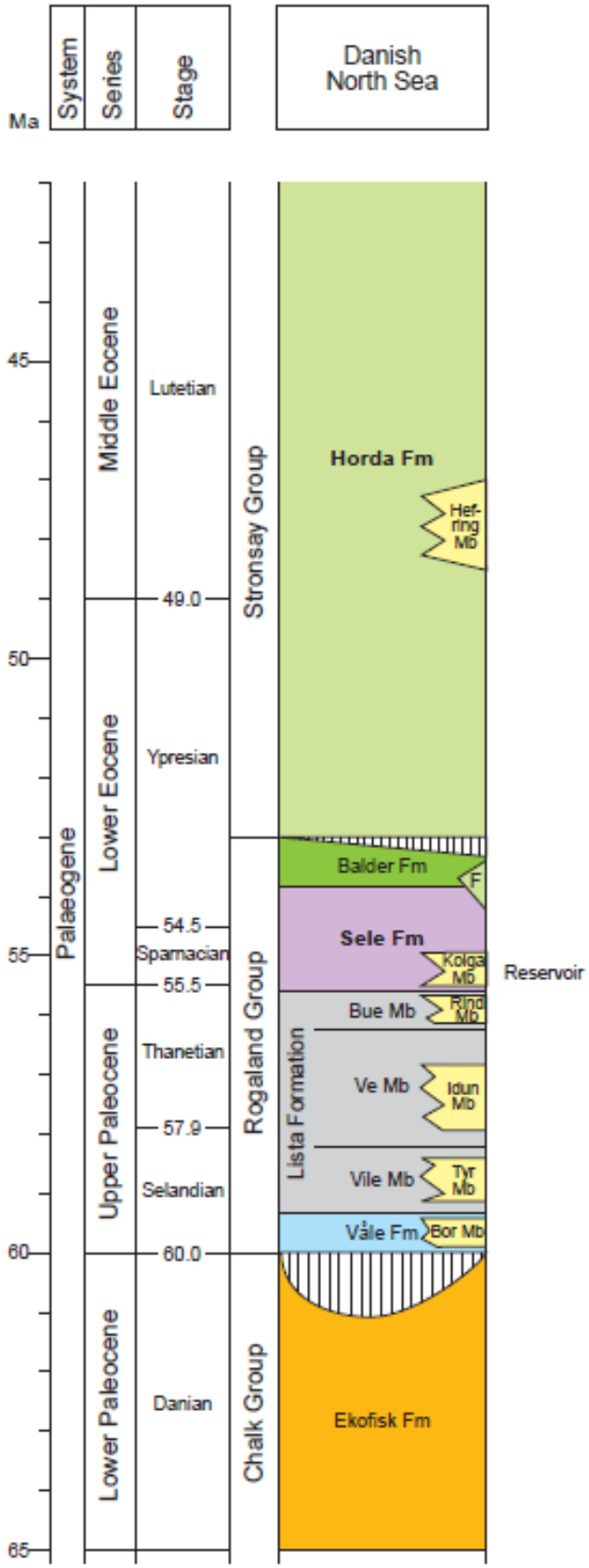

Figure 2. Lower Palaeocene to Middle Eocene lithostratigraphy in the Nini area (Modified from Schiøler et al., 2007 and Petersen et al., 2022).

The Nini West Field is located on the western flank of the Nini anticlinal structure formed by salt tectonics (Danish Energy Agency, 2014) (Figure 1). It forms part of the Nini accumulation that occurs in a combined structural and stratigraphic trap. The reservoir is of Palaeocene-Eocene age and is constituted by the Kolga Member sandstones that have been remobilised into the Balder Formation (Svendsen et al., 2020). The primary seal complex is ~900 m thick and is composed of tight mudstones of the Horda and Lark Formations (Schiøler et al., 2007; Schovsbo et al., 2021; Petersen et al., 2022). The reservoir occurs at a depth of ~1700–1800 m and has a temperature of about 60°C. It consists of fine-grained well-sorted sandstones with quartz and glauconite being the dominant minerals, the latter amounting to 20–30%, while less abundant constituents are feldspars, mica minerals, rock fragments, and heavy minerals (Svendsen et al., 2010; Weibel et al., 2021; Keulen et al., 2022). The glauconite is characteristic of the reservoir. Weibel et al. (2021) showed that the glauconite clasts consist of mixed-layer Fe-smectite/illite and that partially or entirely glauconised minerals of many types occur in the sandstones. Thin rims of cementing phyllosilicates occur on the glauconite clasts.

SAMPLES AND ANALYTICAL METHODS

Stock Tank Oil (STO)

The STO sample (dead oil) was delivered by Ineos and treated and cleaned for impurities at DTU. The STO cleaning procedure includes centrifuging the STO in order to extract dissolved water and passing it through a high-pressure filter (size 7 µm) at room temperature to remove any suspended solid particles.

Samples

The samples analysed in this study are listed in Table 1, and the analytical program is displayed in Figure 3. Apart from the STO, the sample set includes 13 core plugs: three 'fresh' preserved core plugs, three preserved core plugs stored in brine, five plugs cleaned by three different methods, one restored core plug, and one restored then $scCO_2$-flooded core plug. The latter includes two inlet samples with different visual appearances (Figure 4). The core plugs were all collected in the reservoir section drilled by the Nini-4 well in the Nini West Field (Figure 1). The plugs were taken from a depth range from 1774.28 m to 1782.67 m, covering an 8.39 m interval of the formation.

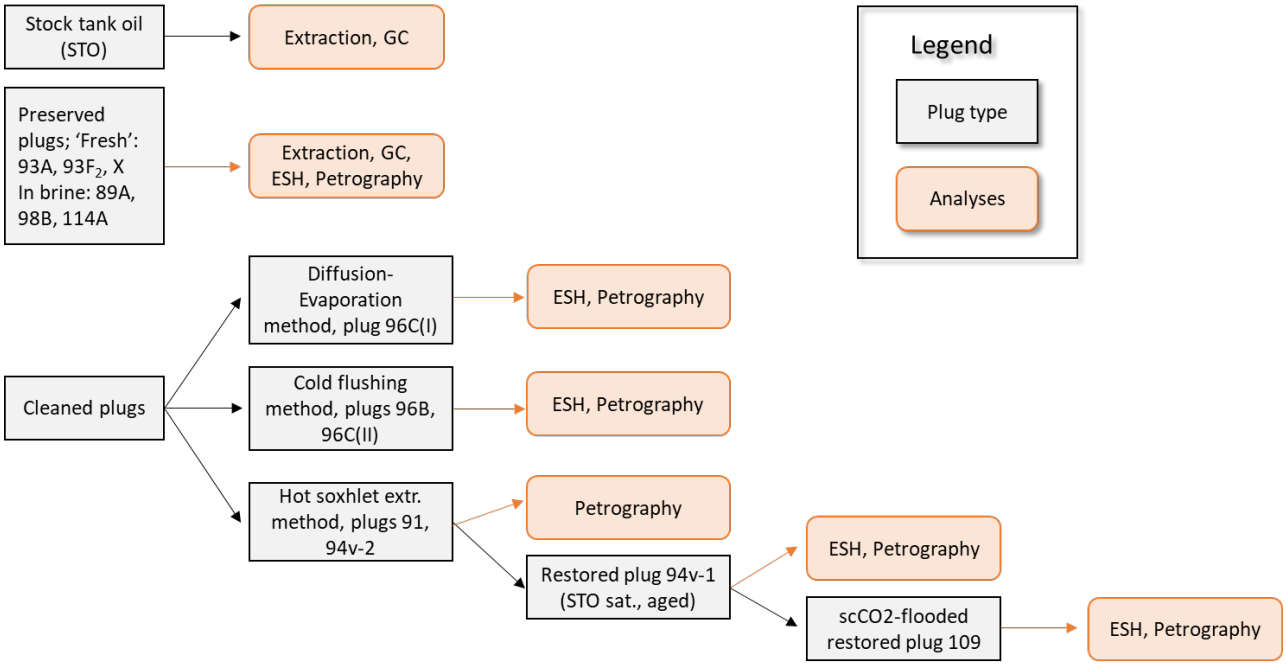

Figure 3. Flow diagram showing the analytical work carried out on the samples. ESH: Extended slow heating pyrolysis; GC: gas chromatography.

Conventional core analysis data, including He-porosity, gas (N_2) permeability and grain density, are available for most of the plugs (GEUS in-house data; MacDonald & Mair, 2003; Table 2). However, no measured data are available for plugs X and 98B, and the data from the nearest plugs were used to interpolate the values. The porosity is very much alike for all plugs varying from 35.00–35.83% except for plug 98B, where the data comes from the nearest plug with a porosity of 33.80%. Permeability shows a broader range, but most plugs have good permeabilities from approximately

1059 mD to 1249 mD. The grain density for all plugs ranges from 2.690 g/cm^3 to 2.716 g/cm^3, a typical value for these sandstones.

Table 1 List of the samples (core plugs) and conducted analyses.

Sample type	Description	Plug	Depth, m (measured)	Extraction and/or MPLC	GC	ESH	Organic petrography
Oil	Stock tank oil (dead oil)	-	-	X	X		
Preserved	Preserved plug, 'fresh'	93A	1775.78			X	
	Preserved plug, 'fresh'	93F$_2$	1775.97			X	
	Preserved plug, 'fresh'	X	1776.9	X	X	X	X
	Preserved plug in brine	89A	1774.28			X	
	Preserved plug in brine	98B	1777.27	X	X	X	X
	Preserved plug in brine	114A	1782.67			X	
Cleaned	Diffusion-evaporation, GEUS	96C(I)	1776.88			X	X
	Cold flushing cleaned, GEUS	96B	1776.85			X	X
	Cold flushing cleaned, GEUS	96C(II)	1776.88				X
	Hot Soxhlet extraction, RRI	91	1775.04			X	X
	Hot Soxhlet extraction, RRI	94v-2	1776.11			X	X
Restored	Hot Soxhlet extraction (RRI), STO sat., aged 1 mth	94v-1	1776.11			X	X
scCO$_2$ flood.	CO2 flooded, STO sat. + aged, inlet A	109	1781.04			X	X
	CO2 flooded, STO sat. + aged, inlet B	109	1781.04			X	X

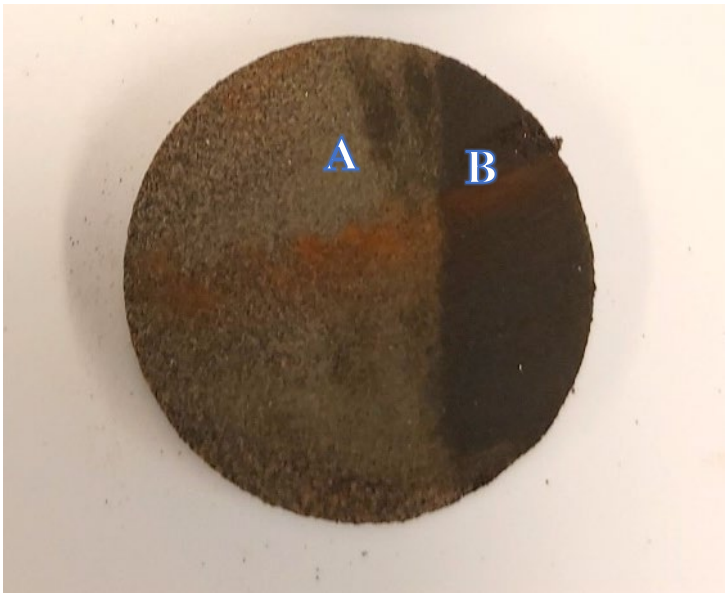

Figure 4. A cylindrical sample was taken from the inlet of core plug 109 after scCO$_2$ flooding. The sample was cut into two pieces, A and B, depending on the colour difference.

Table 2. Petrophysical properties of the core samples reported in the CCAL report (MacDonald and Mair, 2003).

Sample type	Description	Plug ID	Depth m	Porosity %	Gas perm. mD	Grain density g/cm^3	Diameter cm
Preserved	Preserved plug, 'fresh'	93A	1775.78	35.11	1064.79	2.702	3.75
	Preserved plug, 'fresh'	93F$_2$	1775.97	35.00	1058.91	2.707	3.75
	Preserved plug, 'fresh'	X	1776.90	35.05*	1325*	2.695*	3.75
	Preserved plug in brine	89A	1774.28	35.73	813.07	2.707	3.71
	Preserved plug in brine	98B	1777.27	33.8*	1080*	2.69*	3.75
	Preserved plug in brine	114A	1782.67	35.23	768.60	2.699	3.64
Cleaned	Diffusion-evaporation, GEUS	96C(I)	1776.88	35.39	1212.29	2.712	3.73
	Cold flushing cleaned, GEUS	96B	1776.85	35.46	1248.73	2.711	3.74
	Cold flushing cleaned, GEUS	96C(II)	1776.88	35.39	1212.29	2.712	3.73
	Hot Soxhlet extraction, RRI	91	1775.04	35.00	1180.00	2.690	3.73
	Hot Soxhlet extraction, RRI	94v-2	1776.11	35.50	fractured	2.700	3.73
Restored	Hot Soxhlet extraction (RRI), STO sat.	94v-1	1776.11	35.50	fractured	2.700	3.73
scCO$_2$ flood.	CO2 flooded, STO sat. + aged, inlet A	109	1781.04	35.14	1121.51	2.716	3.80
	CO2 flooded, STO sat. + aged, inlet B	109	1781.04	35.14	1121.51	2.716	3.80

* Data not measured on plug but derived from nearest plug

Preserved Plugs

The preserved core plugs were taken from so-called seal peels, which are core pieces that were sealed immediately after drilling by wrapping the core in plastic and aluminium before being embedded in wax (Fig. 5). This is meant to preserve the original fluid composition in the reservoir before, e.g. production starts and alter the initial conditions. Plugs 93A, 93F$_2$ and a plug with no number (hereafter plug X) were taken immediately after opening the seal. In contrast, plugs 89A, 98B and 114A were taken some time before analysis and meanwhile stored in brine in a closed container (Table 1).

Figure 5 Seal peel of the core piece from the Nini-4 well (left). The cored plug was drilled from the seal peel, where oil can be seen saturating the plug (right).

Cleaned Plugs

The three methods used for cleaning the plugs from oil, brine, salts, mud filtrate and contaminants basically go from gentle to harsh:

1. *Diffusion-evaporation method (GEUS)* – The gentlest cleaning method. Plug 96C (hereafter 96C[I]) was cleaned by this method (Table 1). The cleaning occurred by alternating diffusion in toluene and methanol, during which the hydrocarbons are assumed to migrate to the surface of the plug. Between each diffusion cycle, the samples went through evaporation at room temperature.

2. *Cold flushing method (GEUS)* – A more comprehensive cleaning method. Plugs 96B and 96C (hereafter 96C[II]) were cleaned by this method (Table 1). Toluene and methanol were alternately flushed through the plug until no hydrocarbons were visually observed in the effluent (colourless effluent). To ensure the complete removal of salt, silver nitrate solution was added to the methanol effluent while observing any precipitation.

3. *Hot Soxhlet extraction (Robertson Research International, RRI)* – The harshest cleaning method. Plugs 91 and 94v-2 were cleaned by this method (Table 1). The plugs were cleaned by hot Soxhlet extraction using an azeotropic mix of chloroform, methanol, and methylamine, followed by toluene (MacDonald & Mair, 2003). UV light and the solvent colour were used to check the samples for hydrocarbon remnants. Cleaning for hydrocarbons took 7 days, after which toluene was replaced by methanol to remove the formation water and salts.

Restored Plug

A hot Soxhlet extraction cleaned core plug (94v-1; Table 1) was restored. The core plug was saturated with formation water under vacuum followed by saturation reduction by nitrogen using a porous plate to the initial (connate) water saturation (S_{wi}). The core plug was then placed under vacuum for a very short time and submerged with STO to replace the gas with oil, followed by ageing for one month under reservoir pressure (200 bar) and temperature (60°C) conditions. After ageing, the core plug was again flooded with STO. Plug preparation was done at the Core Analysis Laboratory at GEUS.

Supercritical CO_2-flooded Plug

As described above, a restored core plug (109; Table 1) was flooded with $scCO_2$ under reservoir conditions in the Core Analysis Laboratory at GEUS. Plug 109 was the inlet plug of a flooded three-plug composite core. The core plug had a S_{or} of ~19.74%. $scCO_2$ and brine were cyclically injected during 5 cycles at flow rates of 800 ml/h and 100 ml/h, respectively. The residual oil saturation after $scCO_2$ flooding was approximately 4.6%. The outlet sample was divided into two pieces with different visual appearances for analysis (Figure 1).

Analytical Methods and Unit Conversion

Extraction and Gas Chromatography

Two preserved core plug samples, 98B and X, were solvent extracted with CH_2Cl_2/MeOH (93:7 v/v) using a Soxtec system at GEUS (Table 1). The asphaltenes in the extracts were removed by precipitation in 40-fold excess of *n*-pentane. The asphaltene-free extracts were separated into saturated hydrocarbons, aromatic hydrocarbons, and polar compounds by medium-pressure liquid

chromatography (MPLC; Radke et al., 1980). The STO composition was analysed by Applied Petroleum Technology Norway A/S (Slaattedal, 2022). The saturated fractions from the extracts and STO were analysed on a Hewlett Packard 5890 gas chromatograph in the Laboratory of Organic Carbon (LOK) at GEUS.

Extended Slow Heating (ESH) Pyrolysis

A total of 13 samples (including two pieces from plug 109) were subjected to the Extended Slow Heating (ESH®) analysis at the Lithospheric Organic Carbon Laboratory (LOC), Department of Geoscience, Aarhus University. The method involves a continuous slow ramp heating pyrolysis of 50 mg of a dry ground sample from 100°C to 650°C at a 10°C per minute rate using a HAWK Pyrolysis and TOC analyser (Wildcat Technologies). The amounts of hydrocarbons released during the pyrolysis were measured in real-time by an in-line FID detector. The hydrocarbon pyrogram was integrated following the proprietary ESH Slice&Dice® algorithm, in which the increasing pyrolysis temperature corresponds to an increase in the molecular size of the hydrocarbons and hence the specific gravity of the corresponding population of oil. The densities of the oil fractions determined by ESH are light oil, 0.773 g/cm^3; mobile oil, 0.807 g/cm^3; semi-mobile oil, 0.899 g/cm^3; immobile oil, 1.022 g/cm^3; solid bitumen/asphaltenes, 1.2 g/cm^3. The API was accordingly estimated using the propriety calibration of the ESH pyrogram with oil standards of known specific gravity and API. Apart from the above oil fractions, minor amounts of C=O organic bonds in polar/asphaltene compounds were determined.

Unit Conversion: Saturation Estimate and Porosity Correction

The outcome of the ESH pyrolysis is a weight percentage (wt.%) representing the fraction of each type of hydrocarbon to the total amount of sample (rock and hydrocarbon while neglecting water). The volume percentage (vol.%) is convenient for representing the amounts of hydrocarbons for each gram of rock, which is not sufficient in describing the correlation between the quantities of hydrocarbons and the physical flow properties of the rock like the unit system of saturation percentage used in reservoir engineering. Conducting the ESH analyses on cleaned samples can measure the amount of hydrocarbon which cannot be removed for each cleaning method, causing an underestimation of the porosity when measured using a He-porosimeter. In this section, the derivation to convert the results of ESH from vol.% to saturations is presented, followed by the derivation of the equation required to correct the He-porosimeter porosity measurement based on the results of the ESH from cleaned core plugs.

The outcome of the ESH pyrolysis is a wt.% or vol.% of each type of hydrocarbon fraction to the total amount of sample (rock and hydrocarbons) while neglecting the water and gas content. Which reads:

$$Vol.\%\ (i) = \frac{V_i}{V_R + \sum_{i=1}^{n} V_i} 100\%$$

Here V is volume and has the unit of $[L^3]$, while the subscript R is rock and i is the i^{th} species of the hydrocarbons. This means that for each 100 ml of the sample, there is $Vol.\%(i)$ ml of hydrocarbon i and $100 - \sum_{i=1}^{n} V_i$ ml rock. On the other hand, the saturation, S, of species i is defined as the percentage of the pore volume of which the hydrocarbon i occupies and reads:

$$S_i = \frac{V_i}{V_p}\,100\%$$

Knowing the porosity, ϕ, of the rock sample, which is the fraction of the pore volume, V_p, over the total volume of the rock ($V_p + V_R$), we can calculate the pore volume from the rock volume as follows:

$$V_p = \frac{\phi}{1-\phi} V_R$$

Thus, the saturation of i^{th} hydrocarbon reads:

$$S_i = \frac{Vol.\%(i)}{\frac{\phi}{1-\phi}\left(100 - \sum_{i=1}^{n} Vol.\%\,(i)\right)}\,100\%$$

During a routine core analysis, He-porosity is the industry standard. However, this method assumes the absolute removal of any fluid from the pore space since the technique relies on occupied volume in relation to a reference volume in which the helium gas is allowed to expand within. In the case of partial removal of hydrocarbon, part of the pore volume will still be occupied by hydrocarbons, and the estimated pore volume is less than the actual value. Similarly, the rock volume is overestimated, and the difference between the actual and measured volumes is equal to the hydrocarbon volume causing the porosity to be underestimated. Thus, the measured porosity, ϕ_m, measured by the He-porosimeter, can be expressed as:

$$\phi_m = \frac{V_p - V_{HC}}{V_T} = 1 - \frac{V_R + V_{HC}}{V_T} = \phi - \frac{V_{HC}}{V_T}$$

The term $-V_{HC}/V_T$ is the correction factor needed to be added to the measured porosity. Conducting ESH measurement on a cleaned sample gives the amount of hydrocarbon left in the core sample after cleaning. This value can be used to calculate the error in the porosity measurement and the correction factor as follow:

$$Vol.\%\,(HC) = \frac{V_{HC}}{V_R + V_{HC}}\,100\%$$

, where V_{HC} is equal to the sum of the hydrocarbon volume fraction, $\sum_{i=1}^{n} V_i$

Dividing both the nominator and the denominator with the total volume, the previous equation reads:

$$Vol.\%\,(HC) = \frac{V_{HC}}{V_T}\frac{V_T}{V_R + V_{HC}}\,100\%$$

Thus, the correction factor reads:

$$\frac{V_{HC}}{V_T} = Vol.\%\,(HC) * \frac{V_R + V_{HC}}{V_T} = Vol.\%\,(HC) * (1 - \phi_m)$$

In addition to correcting the measured porosity, the method can be used to judge the efficiency of the cleaning method and hence the best method to clean the specific rock sample.

Organic Petrography

Polished pellets suited for incident light microscopy were prepared for 14 samples (Table 1). The remaining oil and solid bitumen/asphaltens were examined in reflected white light and blue and UV light illumination at GEUS and LOC using Zeiss microscopes.

LIQUID OIL AND SOLID BITUMEN: OPTICAL PROPERTIES AND IDENTIFICATION

Microscopic identification of the liquid and solid oil remaining in the Nini reservoir relies on optical properties, including morphology, reflectance and colour in white reflected light, and fluorescence intensity and colour in blue and UV light illumination. The oil can be grouped into two main classes: (1) Liquid oil and (2) solid hydrocarbons.

(1) Liquid oil includes oil droplets, oil films, exudates, and oil dissolved in the embedding resin (Alpern et al., 1992). Optical observation of liquid oil in sedimentary rocks, in particular source rocks and coals, has been documented for decades, e.g. by Teichmüller (1974), Hagemann and Hollerbach (1986), Pradier et al. (1990), Alpern et al. (1992), Kus et al. (2016), Petersen (2017), and Goodarzi et al. (2018), but no formal classification has been established. The following oil types were identified in the Nini West reservoir:

- Oil droplets occur as isolated or clusters in the mineral matrix and trapped in the embedding resin of the pellet. The outline of the droplets may change during illumination by blue light.

- Exudates are more diffuse in optical appearance and commonly emerge from small orifices in the rock matrix during blue light excitation.

- Oil oozes are likewise diffuse and usually occur as haze-like films in the rock matrix.

- Increased fluorescence intensity of the embedding resin may indicate the presence of dissolved oil, which according to Alpern et al. (1992), is saturated hydrocarbons. In contrast co-existence of oil droplets and oil films suggest the presence of aromatic oil not soluble in the resin.

The fluorescence colour and intensity of the oils are related to the oil quality, i.e., oil density (API) and viscosity (Stasiuk & Snowdon, 1997). Under blue light illumination, the fluorescence colour changes with increasing maturity from yellow and orange brownish of heavy and degraded oils, over greenish-yellowish in lower mature, more aromatic and polar oils, to bluish in mature paraffinic light oils and condensates (Hagemann & Hollerbach, 1986). Small aromatic units show the highest fluorescence intensity, while polyaromatic units and saturated hydrocarbons reveal no significant fluorescence (Hagemann & Hollerbach, 1986; Pradier et al., 1990).

(2) Solid hydrocarbons have been formally described and classified as exsudatinite and solid bitumen (Pickel et al., 2017; Sanei, 2020). Exsudatinite is a secondary maceral and refers to an early, heavy yellowish to orange fluorescing hydrocarbon product generated from liptinite macerals within the incipient oil-generation window *sensu* Sanei (2020). Exsudatinite is thus not considered further in this context. Solid bitumen has been described in numerous publications (e.g. Jacob, 1989; Landis & Castaño, 1995; Mastalerz et al., 2018), but Sanei (2020) presented a new classification of solid bitumen and also described the difference between bitumen and solid bitumen. Part of the solid bitumen identified in this study may be bitumen (asphaltenes) and should likely be included in the so-called 'immobile oil' fraction. Bitumen is a not fully consolidated, highly viscous oil residue that appears dark in white reflected light and can be (partly) extracted by organic solvents (Tissot & Welte, 1984; Hunt, 1996). In the Nini West reservoir, it is likely formed by asphaltene precipitation from the crude oil due to in-reservoir changes, mainly pressure, volume, and temperature (PVT) conditions, e.g. caused by the scCO2 injection (see below).

Solid bitumen is like bitumen formed from the precipitation of asphaltenes due to changing reservoir conditions probably induced by hydrocarbon production over time. Still, in contrast to bitumen, it is consolidated and solidified at reservoir temperature. The identified solid bitumen would, in the classification scheme of Sanei (2020), mainly be equivalent to primary-oil solid bitumen. In the Nini

West reservoir sandstones, the solid bitumen is primarily associated with glauconite clasts, where the presence of solid bitumen is revealed by its dark yellow, orange, to brownish fluorescence under blue light illumination (see below). To a limited extent, the fluorescence may appear from some associated bitumen/asphaltenes. The glauconite itself exhibits no fluorescence.

In the current study solid bitumen/asphaltenes are considered as one group.

RESULTS AND DISCUSSION

Stock Tank Oil (STO) and Preserved Core Extracts

The analyses of the STO and preserved core extracts provide a general characterisation of the remaining oil in the Nini reservoir and serve as a 'baseline' for understanding the data obtained from the clean, prepared and $scCO_2$-flooded plugs.

The preserved core extracts were derived from plug X, which was freshly drilled from an opened seal peel, and plug 98B, which had been stored in brine (Table 1). The bulk geochemical composition of the extracts and the STO are shown in Table 3. The extracts are relatively similar in composition, with a dominance of polar compounds followed by saturated hydrocarbons. The asphaltene content is fairly high. The STO is not unexpectedly more paraffinic and contains much lower contents of asphaltenes and polar compounds, while the aromatic fraction is higher (Table 3).

The Nini-4/4a well was drilled with oil-based drilling mud (OBM) containing base oil EDC 95/11 which has a narrow diesel-like range from approximately nC$_{12}$–nC$_{20}$ with a maximum between nC$_{14}$–nC$_{19}$ (Figure 6). Lower and higher n-alkanes are largely absent. The base oil has an API of c. 43° with a white to blue fluorescence colour. According to Geochemical Investigations Ltd (2003), the reservoir interval from 1773.6–1776.7 m has a maximum of 10% contamination. The gas chromatogram of the STO shows slightly enhanced nC$_{15}$–nC$_{16}$ peaks, likely indicating minor contamination of the dead oil (Figure 7). The GC trace of the extract from plug X likewise shows enhanced peaks in the nC$_{15}$–nC$_{18}$ range, which is in line with the EDC 95/11 base oil (Figure 8). In contrast, the GC trace from plug 98B reveals no signs of contamination.

Table 3 Bulk composition of plug extracts and stock tank oil.

SAMPLE/PLUG	X (46480)	98B (46481)	STO (APT)
TYPE	Fresh' plug	Plug stored in brine	Dead oil
DEPTH (M)	1776.90	1777.27	n.d.
%ASPHALTENES	14.65	13.15	2.4
%SATURATES	34.13	33.48	55.4
%AROMATICS	11.06	11.76	24.7
%POLARS (NSO)	54.81	54.75	19.9
SAT, ARO, NSO: NORMALISED TO 100%			

Table 4 Oil compositional data of preserved, cleaned, restored, and $scCO_2$-flooded core plugs.

	Plug	Oil	Light Oil	Mobile Oil	Semimobile Oil	Immobile Oil	Solid bitumen/asph.*	ESH API
	ID	vol.%	vol.%	vol.%	vol.%	vol.%	vol.%	°
Preserved	93A	18.09	0.20	6.28	4.90	1.29	5.26	34
	93F2	16.16	0.17	6.38	4.33	0.99	4.14	36
	X	21.31	0.22	6.12	8.66	2.27	3.98	37
	89A	11.57	0.07	3.91	2.95	0.68	3.80	33
	98B	16.78	0.20	4.91	5.55	2.06	3.98	35
	114A	9.15	0.02	1.72	2.04	0.63	4.56	27
Cleaned	96 (I)	1.88	0.00	0.12	0.09	0.00	1.55	14
	96B	1.41	0.00	0.00	0.00	0.00	1.29	n.d.
	96 (II)	-	-	-	-	-	-	-
	91	1.63	0.00	0.00	0.00	0.00	1.53	n.d.
	94v-2	0.72	0.00	0.00	0.00	0.00	0.67	n.d.
Restored	94v-1	28.39	0.52	9.20	10.01	2.56	5.88	37
$scCO_2$-Flooded	109, inlet A	2.02	0.00	0.00	0.01	0.08	1.86	n.d.
	109, inlet B	1.74	0.00	0.00	0.00	0.04	1.63	n.d.

*Asph.: asphaltenes

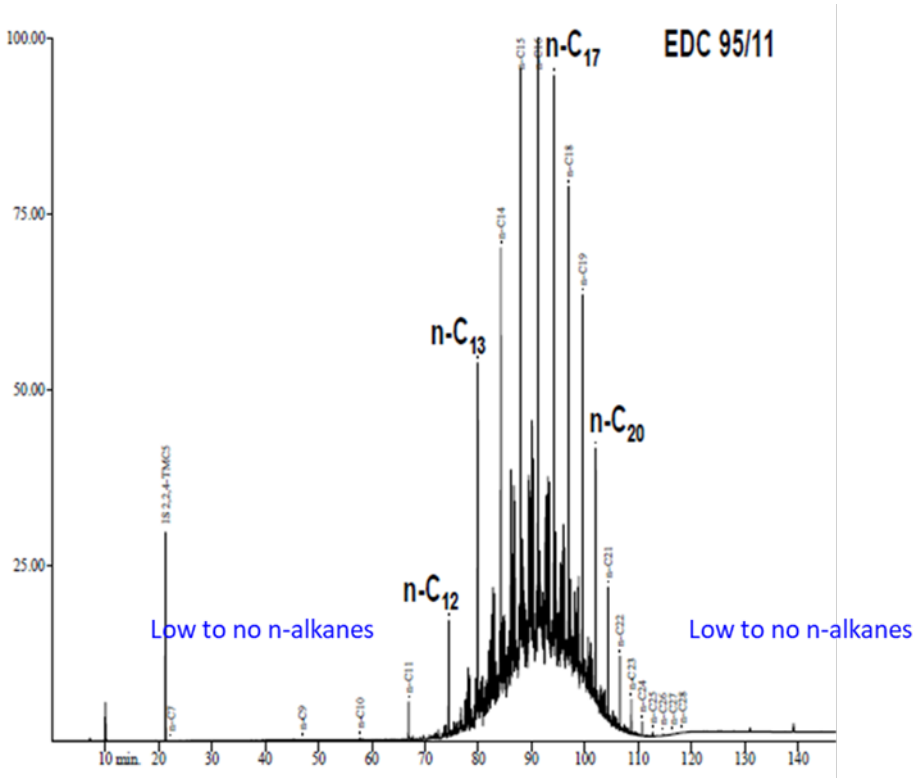

Figure 6 Gas chromatogram of base mud showing *n*-alkanes in the diesel range. The API is 43°, and the fluorescence is white to blue. After Åland et al. (2016).

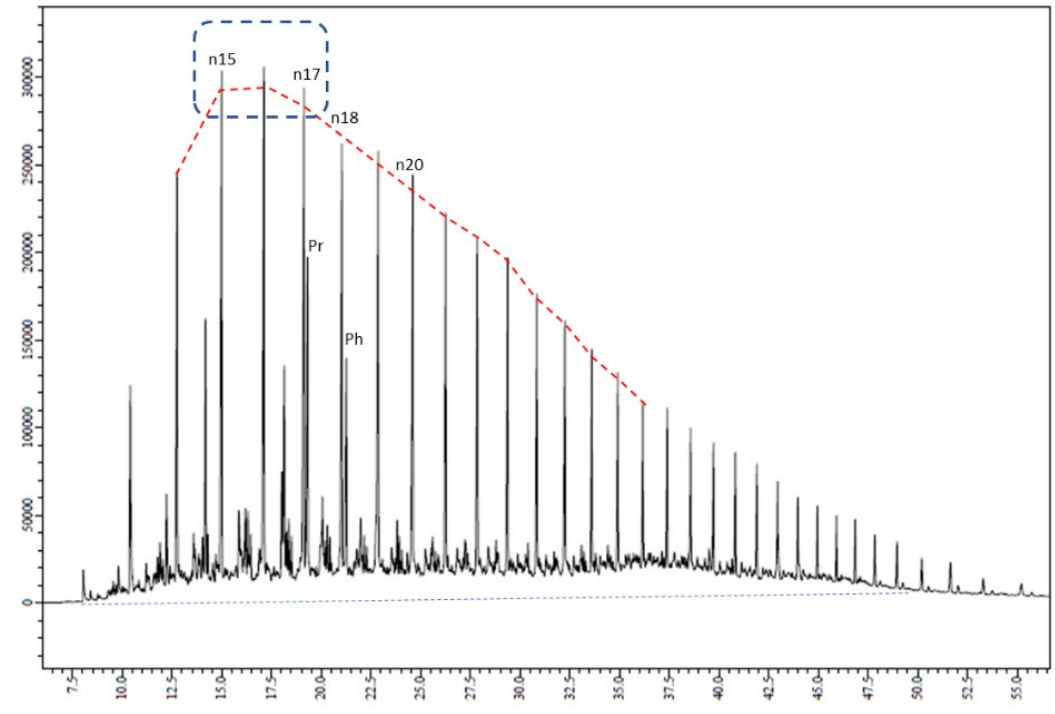

Figure 7. The stock tank oil (STO) gas chromatogram shows slightly enhanced nC$_{15}$–nC$_{17}$ peaks, likely indicating minor contamination from the base mud.

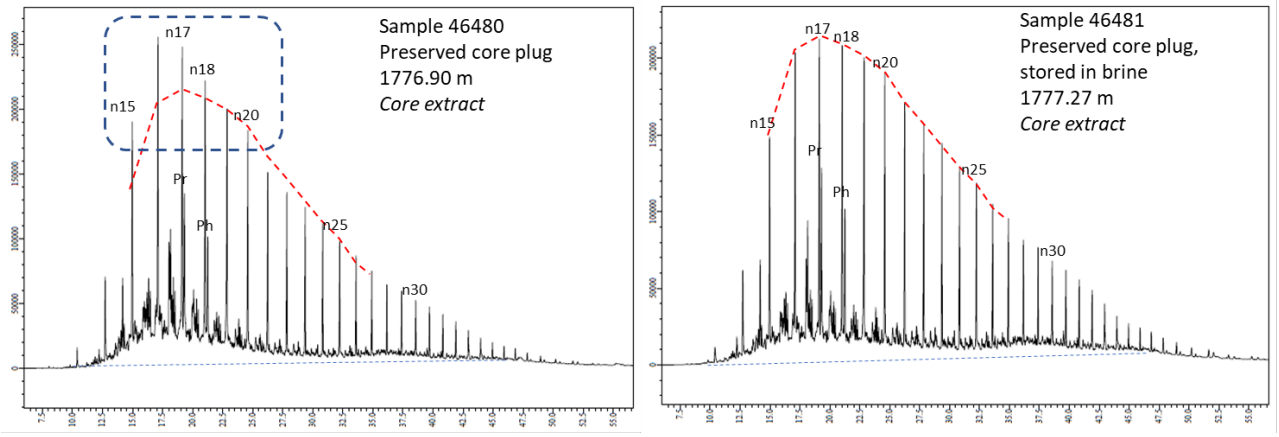

Figure 8. Gas chromatograms of the saturated fraction of the extracts from preserved core plugs. The 'fresh' core plug (left) reveals some contamination in the diesel range, while the core plug that has been stored in brine apparently has no contamination.

A composite photomicrograph taken in white reflected light of the reservoir sandstone shows the textural relationships between glauconite (Gl) clasts, quartz (Qz)/other minerals, and porosity (Po) but also highlights the different visual appearance of the glauconite clasts (Figure 9). The glauconite (Gl) clasts displayed in Figure 9B have different reflectance and colour: one is blackish, and the other dark grey with a faint green glow. The preserved core plugs are saturated with oil that emits a bluish fluorescing colour in UV light (Figure 10). The oil occurs in the porous reservoir matrix and is

dominantly composed of indigenous hydrocarbons (HC), potentially with a minor fraction of base oil. The strong bluish fluorescence from the indigenous hydrocarbons and the base oils prevents a closer observation of the relationship between the hydrocarbons and the mineral matrix of the reservoir, including glauconite clasts. However, in blue light illumination, an orange fluorescence colour of HCs associated with glauconite [Gl(HC)] is to some extent visible, although still blurred by the fluorescence of the indigenous oil ooze (Figure 11). This association of remaining oil and glauconite was confirmed by examining the cleaned and restored plugs (see below).

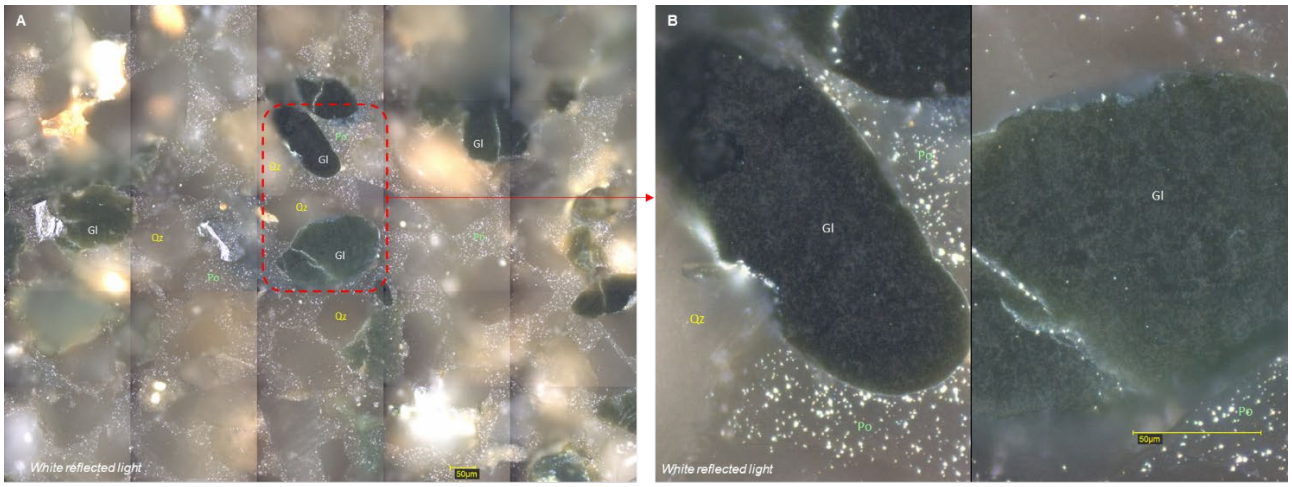

Figure 9. Photomicrographs in white reflected light and oil immersion of the Nini West reservoir. A) Overview photo showing the occurrence of glauconite clasts with varying reflectance in the rock matrix. B) Zoom-in on two glauconite clasts with different reflectance – blackish and greenish. Gl: glauconite; Po: pore; Qz: quartz. Scale bars: 50 µm.

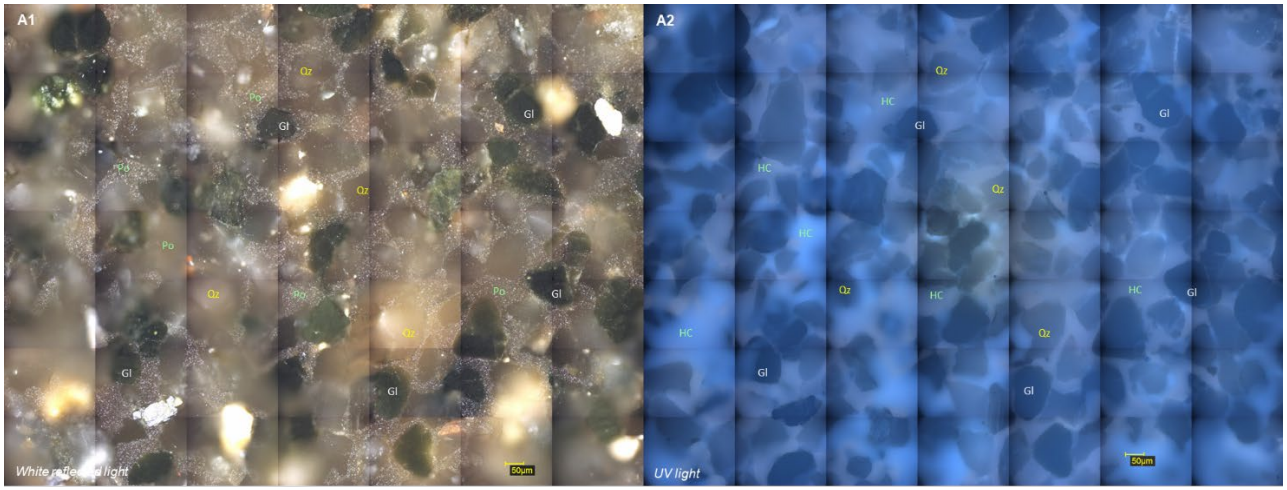

Figure 10. Photomicrographs in oil immersion of the same view of the Nini West reservoir. A1 Abundance of glauconite clasts in the sandstone; white reflected light. A2 The bluish fluorescence is derived from residual oil in the pore space of the sandstone; UV light illumination. Gl: glauconite; HC: hydrocarbon; Po: pore space; Qz: quartz. Scale bars: 50 µm.

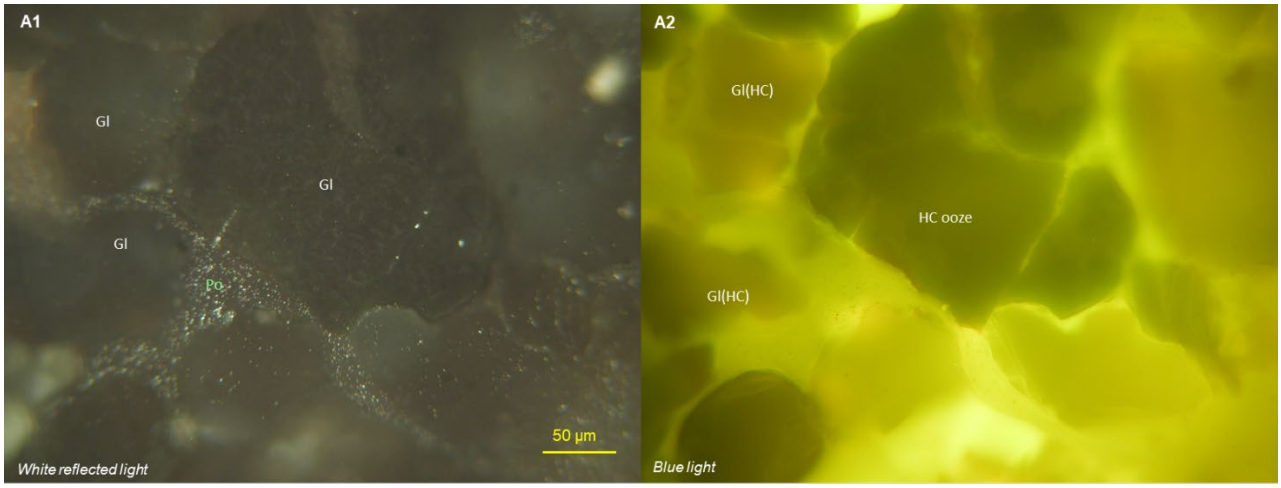

Figure 11. Photomicrographs in oil immersion of the same view of the Nini West reservoir. A1 Abundance of glauconite clasts in the sandstone; white reflected light. A2 Yellowish fluorescing residual oil in the pore space, including hydrocarbon (HC) ooze. The vaguely orange fluorescence of the upper left glauconite clast suggests the presence of heavier oil in the clast [Gl (HC)]; blue light illumination. Gl: glauconite; Gl (HC): glauconite clast associated with hydrocarbons.

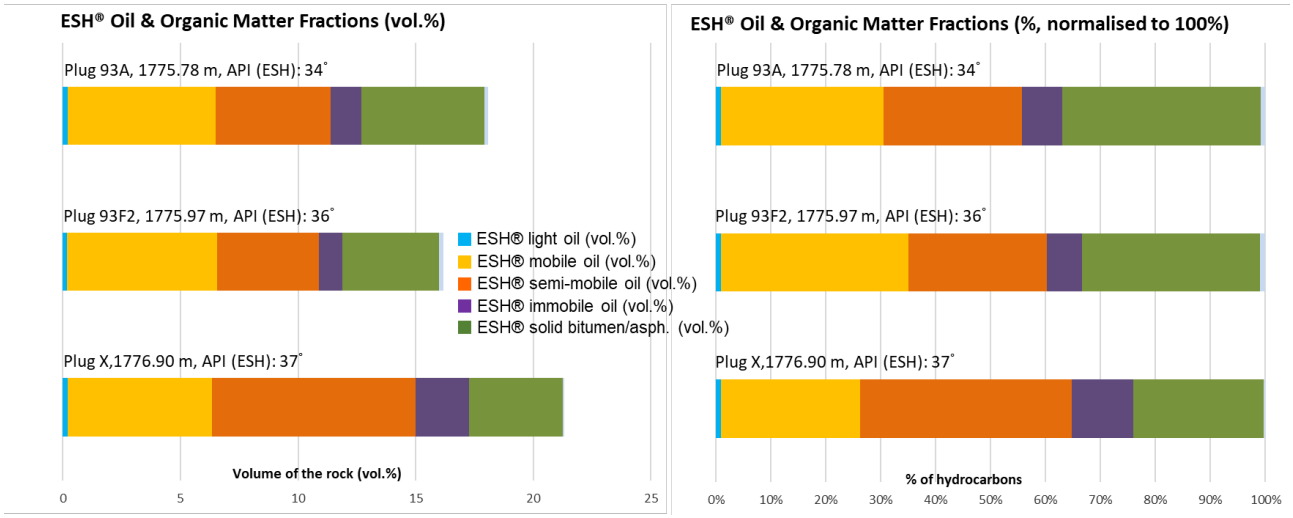

Figure 12. Histograms showing the composition of the remaining oil in the preserved 'fresh' core plugs. Note the appreciable amount of immobile oil and solid bitumen/asphaltenes.

The different oil fractions in several preserved 'fresh' and brine-stored plugs were analysed by ESH, providing the volumes (vol.%) of light oil, mobile oil, semi-mobile oil, immobile oil, and solid bitumen/asphaltenes (Figs. 12 and 13; Table 4). The light oil fraction may be influenced by the base oil contamination. The 'fresh' plugs contain c. 16–21 vol.% oil, while the plugs stored in brine contain less oil (9–17 vol.%). The latter is probably due to brine imbibing into the pore space which can expel some of the oil out of the plug. The reduction in oil in the plugs stored in brine is primarily caused by a smaller fraction of mobile oil, while the immobile oil and solid bitumen/asphaltene fractions are largely unchanged (Figs. 12 and 13; Table 4). The amounts of mobile oil (light, mobile, and semi-mobile oils) range from c. 11–15 vol.% (56–65% normalised) in the 'fresh' plugs suggesting that

most of the oil is movable while a minor fraction is composed of c. 5–7 vol% (35–44% normalised) immobile oil and solid bitumen/asphaltenes (Figure 12; Table 4).

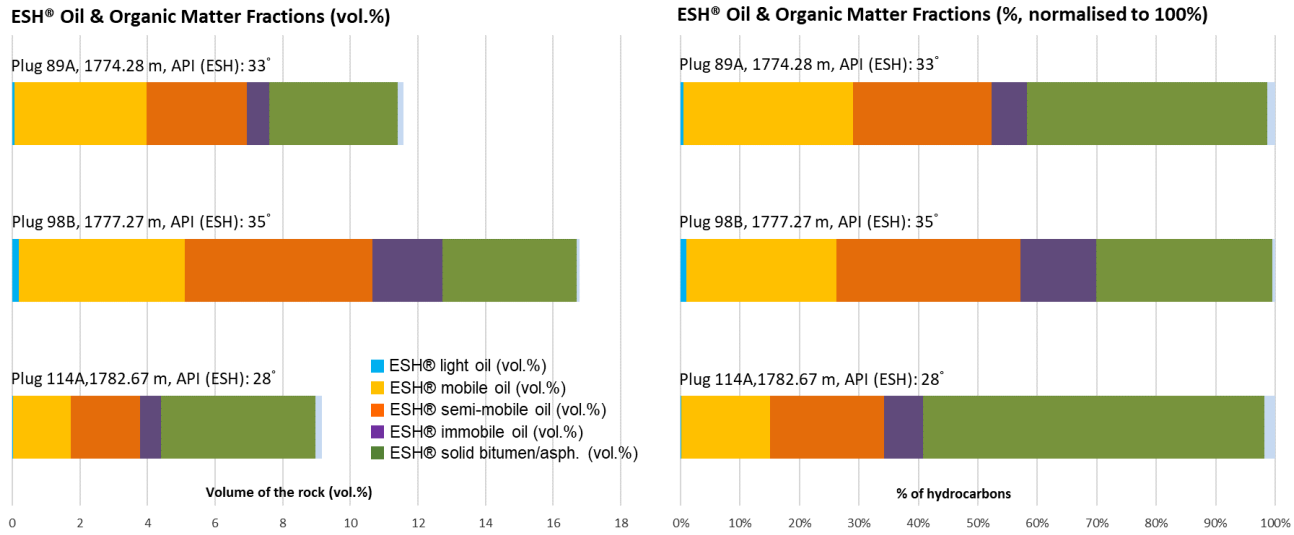

Figure 13. Histograms show the composition of the remaining oil in the preserved core plugs stored in brine. Note the lower quantity of hydrocarbons and considerably higher relative amount of immobile oil and solid bitumen/asphaltenes compared to the 'fresh' plugs. See also Table 4.

The estimated (from ESH) API for the oil from the 'fresh' core plugs ranges from 34°–37° which is close to the measured crude oil APIs ranging from 36.8°–39.2° (Dong E&P, 2003) (Figure 12; Table 4). The lower amount of the relatively lighter mobile oil fractions is reflected in lower estimated API values of 28°–35° of the brine-stored plugs (Figure 13; Table 4). This may suggest that the oil in 'fresh' taken preserved core plugs compositionally are more comparable to the crude oil than preserved plugs stored for some time in brine-filled containers. The latter suffers from the loss of part of the lighter oil fractions due to expulsion caused by gravity segregation; however, it is noteworthy that the immobile oil and solid bitumen/asphaltene fractions remain unaffected. Plugs stored in brine can thus be used for studying the heavier residual oil fractions, e.g. in the context of $scCO_2$ injectivity.

Concluding Remarks

The contamination appears to be minor and restricted to the diesel range, and it will, therefore, not affect the heavy oil fraction $>nC_{20}$. Potential clogging issues will thus relate to the pristine oil in the reservoir. Most of the remaining oil is mobile, e.g., in the CO_2 plume solution. A minor fraction of the remaining oil is non-mobile and may thus have a potentially adverse effect on $scCO_2$ injectivity by clogging the pore network in the reservoir. Likewise, asphaltenes may potentially be a concern due to asphaltene precipitation, which also could have an adverse clogging effect on CO_2 injectivity (see section on $scCO_2$-flooded plug).

Cleaned Plugs

The microscopic examination and ESH pyrolysis of plug 96C(I) demonstrate that the cleaning in methanol and toluene has not effectively removed all hydrocarbons (Table 4). As these seemingly are insoluble in organic solvents, they are regarded as heavy (immobile) oil and solid bitumen/asphaltenes, which are primarily associated with glauconite. The glauconite clasts (Gl) appear greenish to blackish in white reflected light and show internal variations in reflectance, likely related to varying degrees of diagenesis and/or diagenetic origin (Figure 14). The glauconite clasts do not fluoresce, but the associated heavy oil yields a brownish-orange fluorescence colour demonstrating its presence as coatings on the glauconite and in the interior of the glauconite clasts (Gl(SB)) (Figure 14). In some glauconite clasts, the immobile oil or solid bitumen/asphaltenes do not occur in the interior of the glauconite clasts but only in cracks at the surface (Figure 14B, C). Some of the glauconites are derived from mica, showing a microlaminated structure (Figure 14D). Variations in fluorescence intensity/colour may relate to glauconite texture and the degree to which the heavy oil was dissolved during solvent extraction. The brownish fluorescence colour of the hydrocarbon coatings suggests these were most affected by extraction leaving behind solid bitumen/asphaltenes, while the brighter orange interior suggests these hydrocarbons were less affected. The ESH data reveals that the diffusion-evaporation cleaning method has been quite effective. However, although solid bitumen/asphaltenes (1.55 vol.%) are dominant, the plug also contains a minor fraction of mobile and semi-mobile oil (Figure 15; Table 4). The presence of a minor mobile oil fraction in plug 96C(I) is also suggested by the yellowish fluorescence colour of the matrix (Figure 15).

The cold flushing cleaning method is more thorough than the diffusion-evaporation method. Aligned with this, the ESH of plug 96B shows that all mobile oil has been extracted, and only a minor fraction (1.29 vol.%) of solid bitumen/asphaltenes have been left behind (Figure 16; Table 4). In both plugs 96B and 96C(II) the solid bitumen/asphaltenes are primarily associated with glauconite clasts, and it occurs as surface coatings and in small cracks at the glauconite surface and was only rarely observed in the interior of the glauconite clasts (Figure 17). Glauconised mica (Gl[m]) observed in abundance in plug 96C(II) but also in 96B commonly shows retained oil between the laminae of the mineral (Figure 18). During blue light illumination, hydrocarbons are often exuding from the laminae suggesting some degree of oil mobility (Figure 18A, B). However, exudates were not observed from all glauconised mica with remaining oil (Figure 18C, D). The darker orange to brownish fluorescence may indicate that the oil is heavier and likely immobile solid bitumen/asphaltenes (Figure 18C).

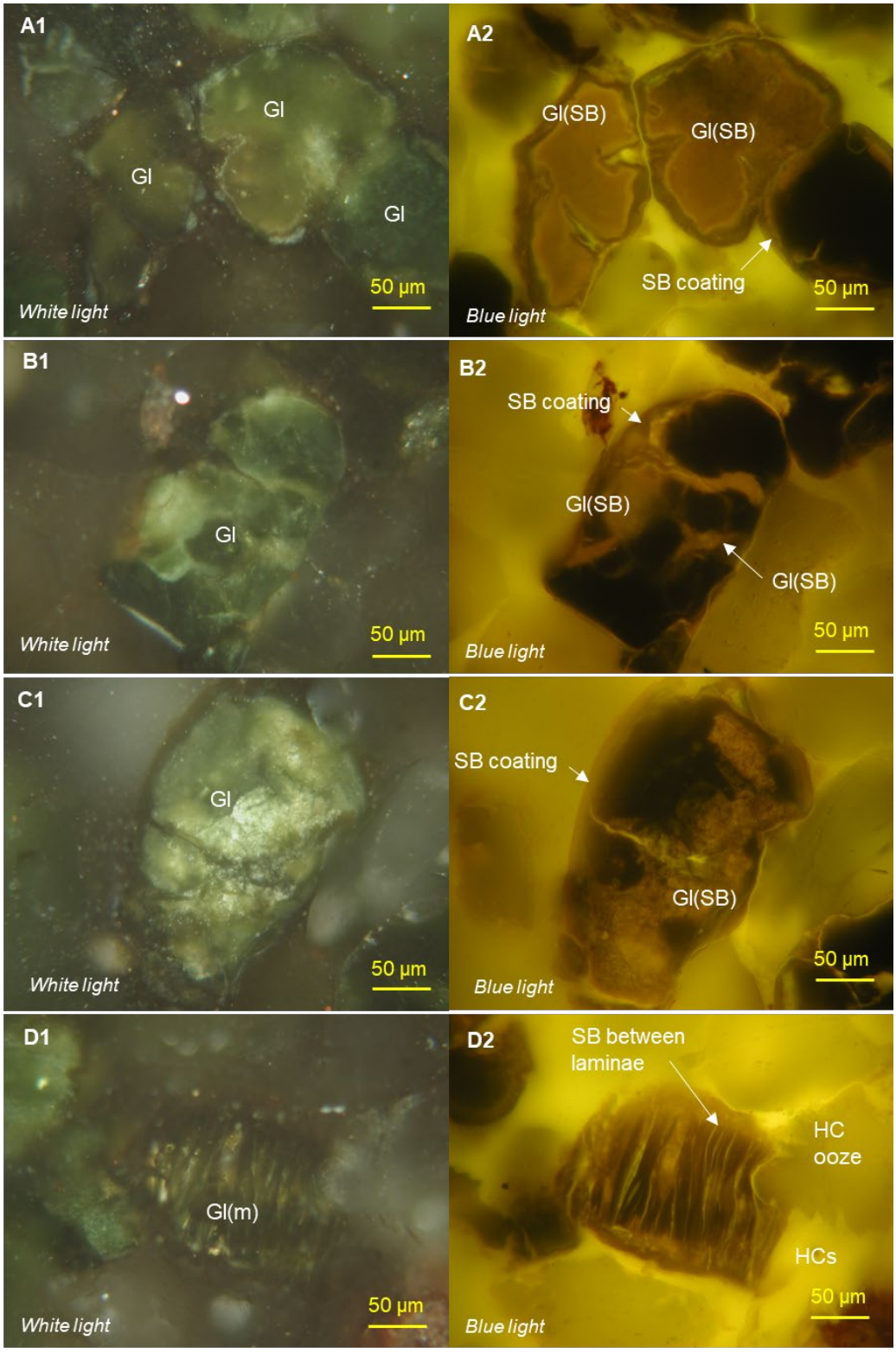

Figure 14. Photomicrographs in oil immersion of remaining oil in plug 96C(I) after cleaning with the diffusion-evaporation method. Orange-brownish solid bitumen/asphaltenes (SB) are observed in the interior of glauconite clasts (Gl [SB]), as glauconite surface coatings, and between the laminae of glauconised mica (Gl[m]). A1–D1: reflected white light; A2–D2: blue light illumination.

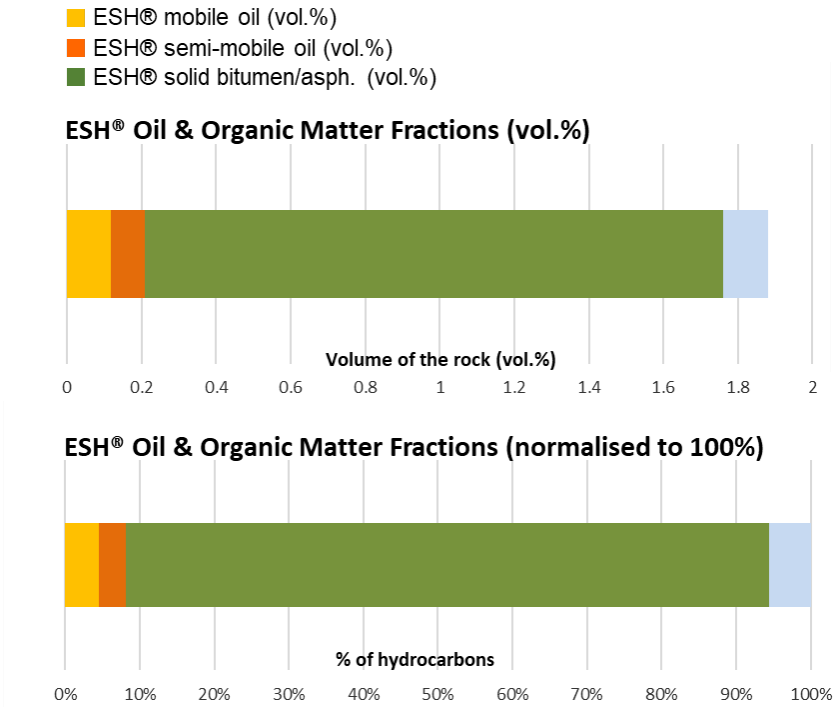

Figure 15. Histograms showing the composition of the remaining oil in the diffusion-evaporation cleaned plug 96C(I) containing mainly solid bitumen/asphaltenes and a minor amount of mobile and semi-mobile oil. Most of the remaining oil has thus been extracted. See also Table 4.

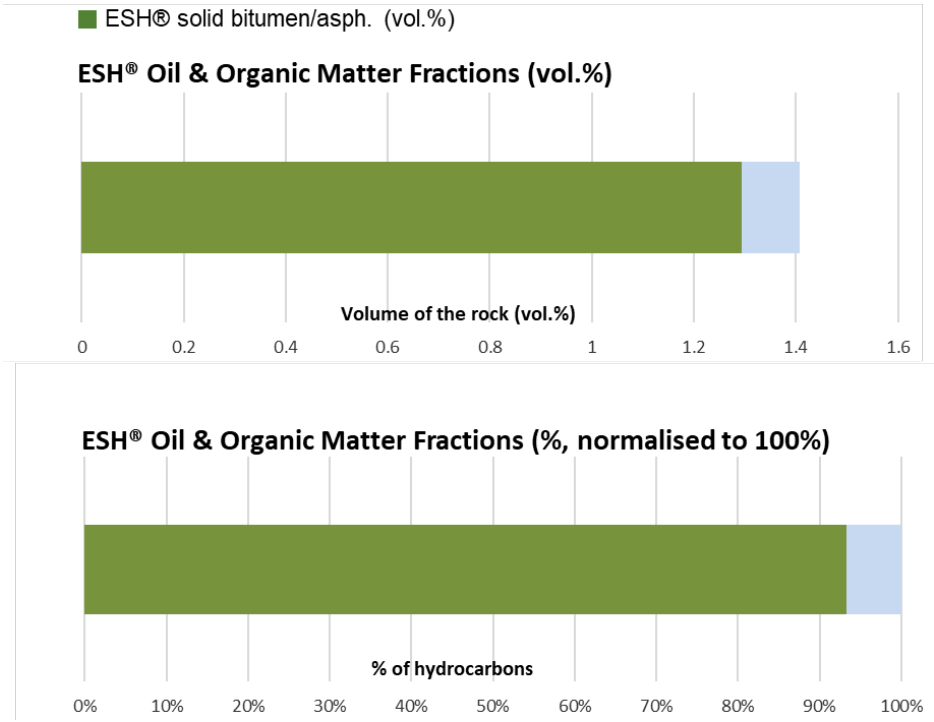

Figure 16. Histograms showing the composition of the remaining oil in plug 96B cleaned by the cold flushing method. All mobile oil fractions have been extracted, and the residual oil consists entirely of solid bitumen/ashaltenes. See also Table 4.

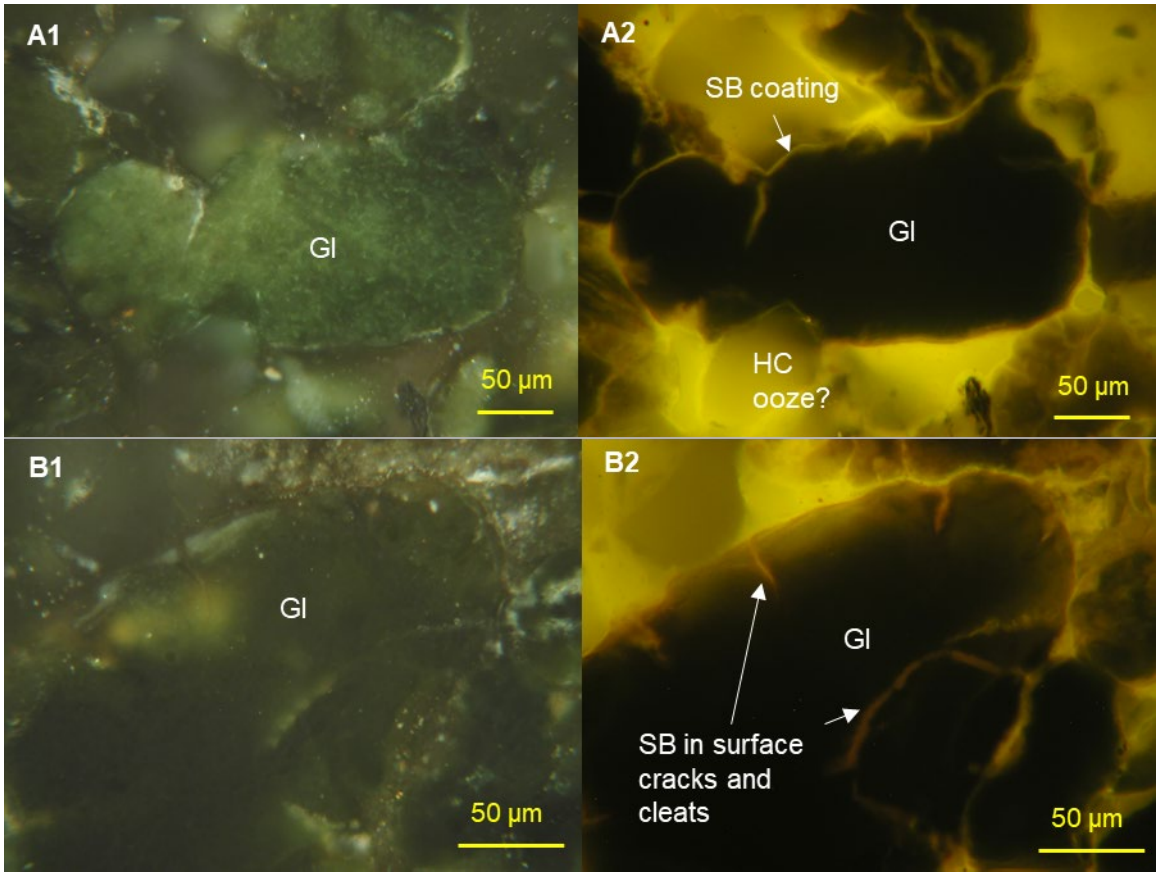

Figure 17. Photomicrographs in oil immersion of remaining oil in plug 96C(II) after cleaning by cold flushing. Remains of orange-brownish solid bitumen/asphaltenes (SB) are observed at the surface and in small surface cracks of glauconite clasts (Gl). A1, B1: reflected white light; A2, B2: blue light illumination.

Hot Soxhlet extraction is the harshest cleaning method and has efficiently cleaned plugs 91 and 94v-2 for remaining oil. In plugs 91 and 94v-2, all mobile oil has been removed, and the remaining oil is composed of 1.53 vol.% and 0.67 vol.% solid bitumen/asphaltenes, respectively (Figure 19; Table 4). Some of the glauconite clasts in plug 91 sill contain solid bitumen/asphaltenes in the interior, while none of the glauconite clasts in plug 94v-2 show fluorescence under blue light illumination, suggesting very efficient cleaning for remaining oil (Figures 20 and 21). In plug 94v-2, only minor remains of solid bitumen/asphaltenes are visible at the surface and in small cracks of the glauconite surface (Figure 20).

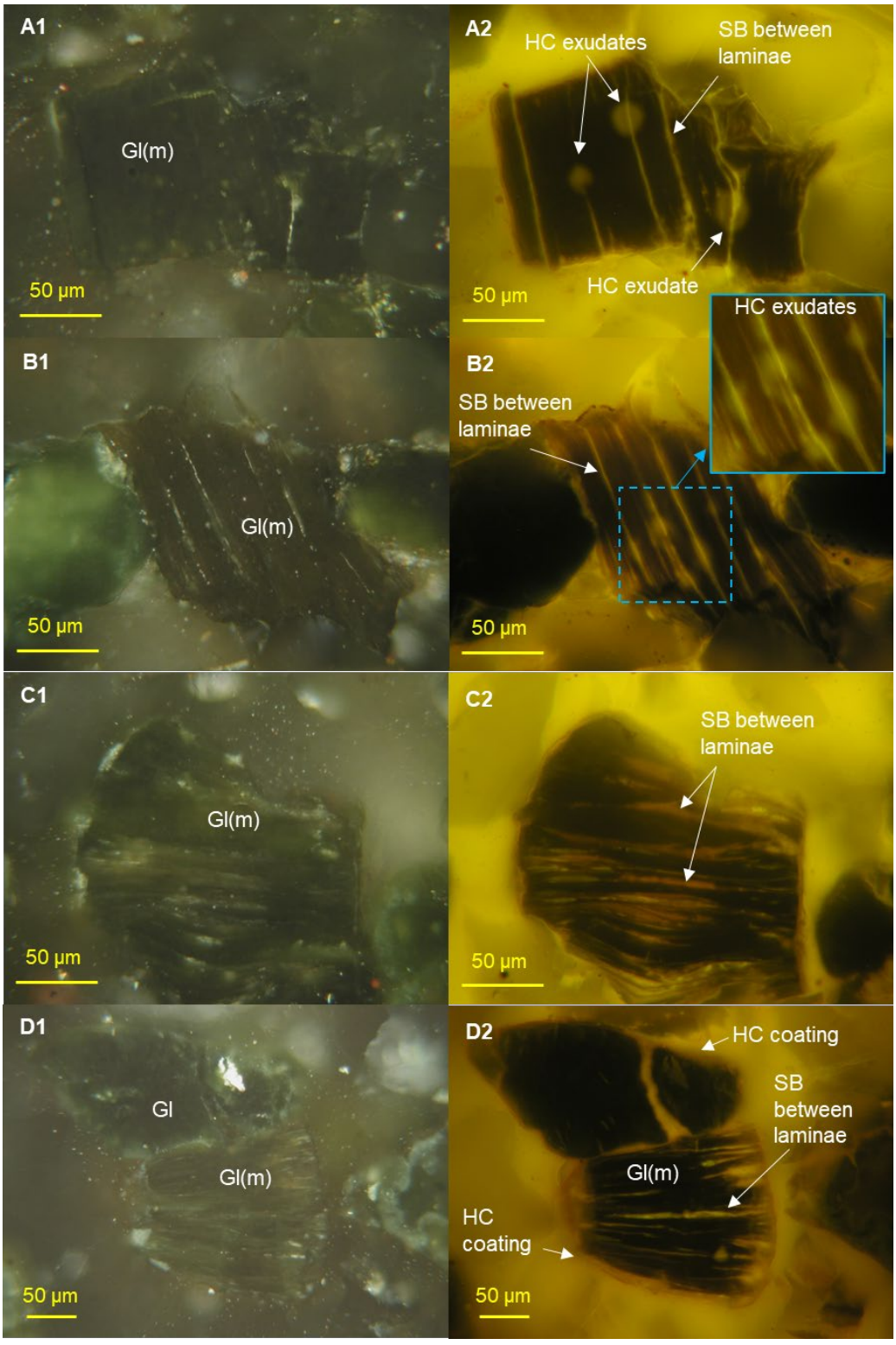

Figure 18. Photomicrographs in oil immersion of remaining oil in glauconised mica (Gl[m]) in plugs 96B and 96C(II) after cleaning with the cold flushing method. Orange-brownish solid bitumen/asphaltenes (SB) are together with HC exudates observed between the laminae of the glauconised mica. A1–C1: reflected white light; A2–C2: blue light illumination. A–C: Plug 96C(II); D: Plug 96B.

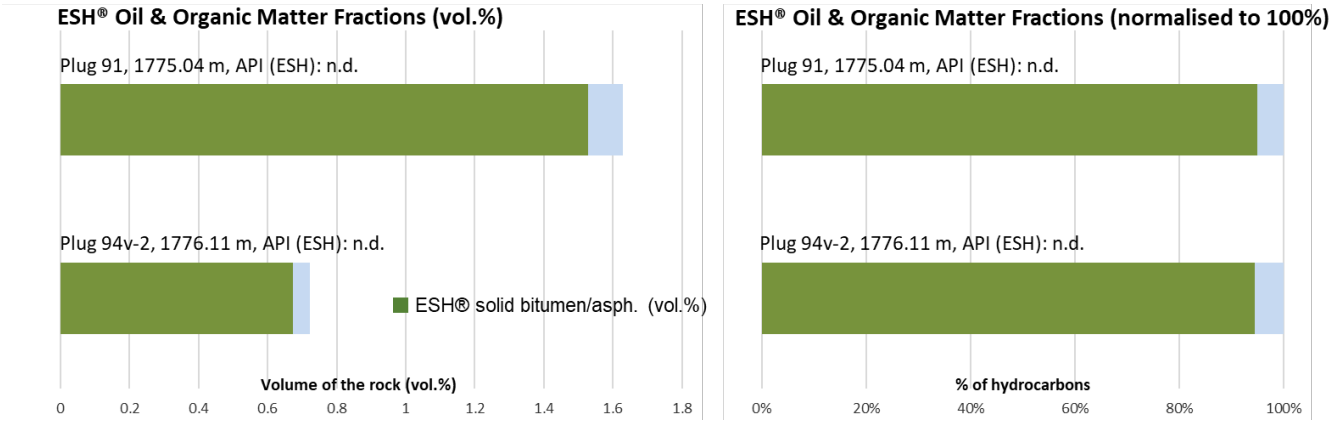

Figure 19. Histograms showing the composition of the remaining oil in plugs 91 and 94v-2 cleaned by the hot soxhlet extraction method. All mobile oil fractions have been extracted, and the remaining oil consists entirely of a minor quantity of solid bitumen/asphaltenes. See also Table 4.

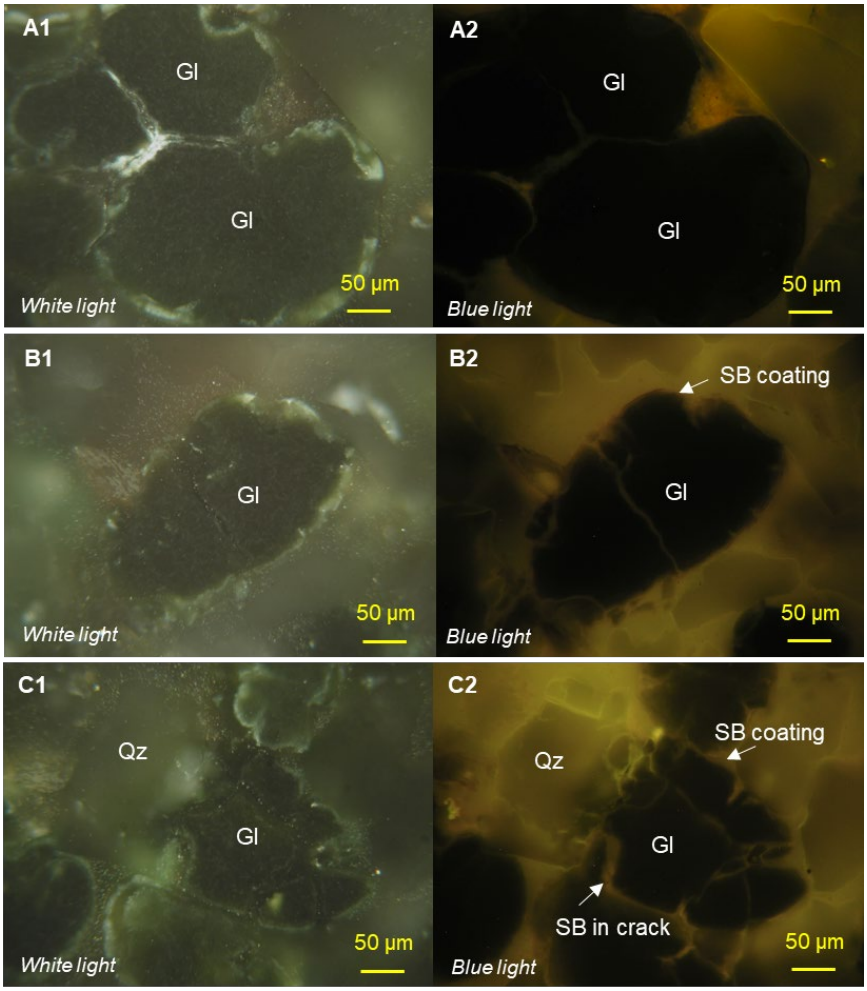

Figure 20. Photomicrographs in oil immersion of remaining oil in plug 94v-2 cleaned by the hot Soxhlet extraction method. No hydrocarbons are observed in the interior of the glauconite clasts (Gl). Remnants of brownish fluorescing solid bitumen/asphaltenes (SB) at the surface and in small surface cracks of the glauconite are observed. A1–C1: reflected white light; A2–C2: blue light illumination.

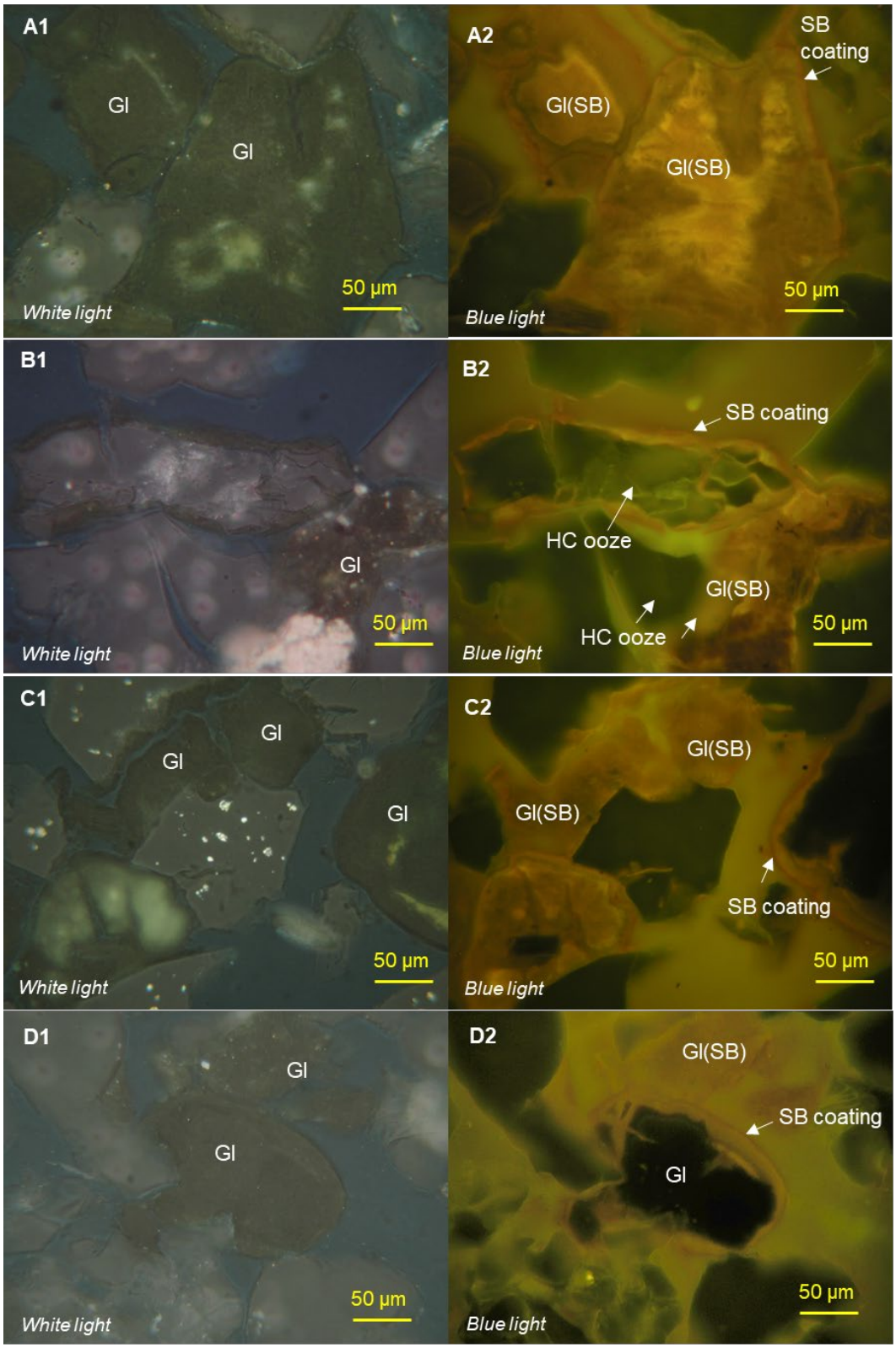

Figure 21. Photomicrographs in oil immersion of remaining oil in plug 91 after cleaning with the hot soxhlet extraction method. Orange-brownish solid bitumen/asphaltenes are observed in the interior of glauconite clasts (Gl [SB]) and as glauconite surface coatings. A1–D1: reflected white light; A2–D2: blue light illumination.

Concluding Remarks

The diffusion-evaporation and cold flushing cleaning methods are gentle and assumed to have a minimal destructive effect on the plugs that will be used for further analyses, e.g. $scCO_2$-flooding experiments. Both methods efficiently remove the oil from the pore space, leaving behind immovable solid bitumen/asphaltenes associated with glauconite that occur principally as surface coatings and in surface cracks/cleats of glauconite and between the laminae of glauconised mica. However, in the case of diffusion-evaporation, a minor mobile oil fraction was not removed. The hot Soxhlet extraction is as efficient as the cold flushing cleaning method. Still, this method could damage the mineral matrix due to the elevated temperature and harsh chemicals, thus altering the original rock structure.

Restored Plug

Plug 94v-1 was initially cleaned by the hot Soxhlet extraction method before being restored to original conditions by STO saturation and ageing. This dramatically changed the composition of the saturating oil. The oil content is 28.39 vol.%, and altogether the quantity of oil is higher than in the preserved core plugs, primarily due to a higher fraction of mobile and semi-mobile oil amounting to 19.73 vol.%, but also higher quantities of immobile oil and solid bitumen/asphaltenes (Figure 22; Table 4). The estimated API is 37° which is completely aligned with the measured API values (Dong E&P, 2003).

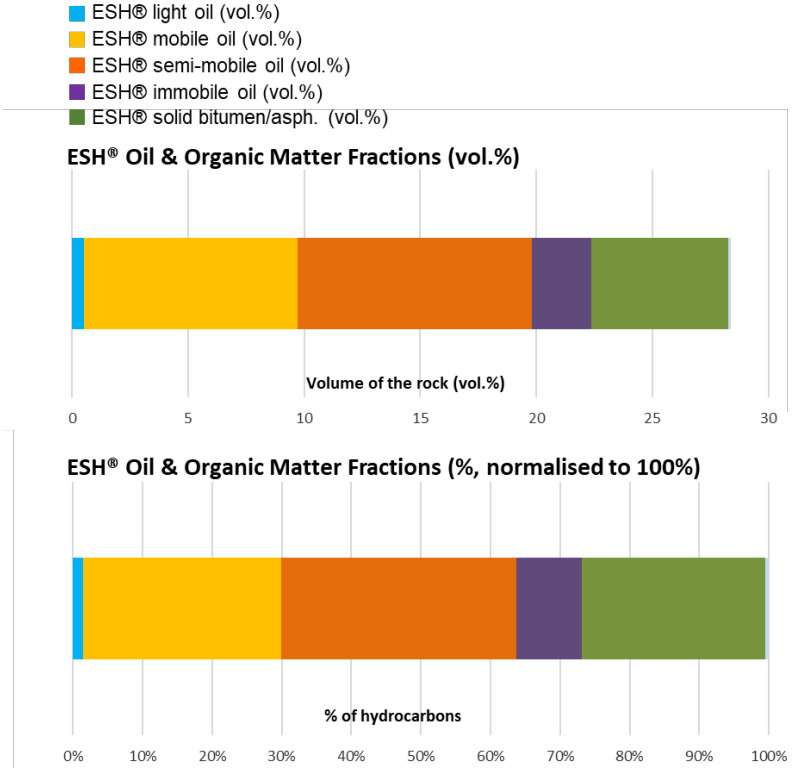

Figure 22. Histograms showing the composition of the oil in the restored (stock tank oil saturated and 1 month aged) plug 94v-1. Note the considerable amount of mobile oil, but also a substantial amount of immobile oil and solid bitumen/asphaltenes.

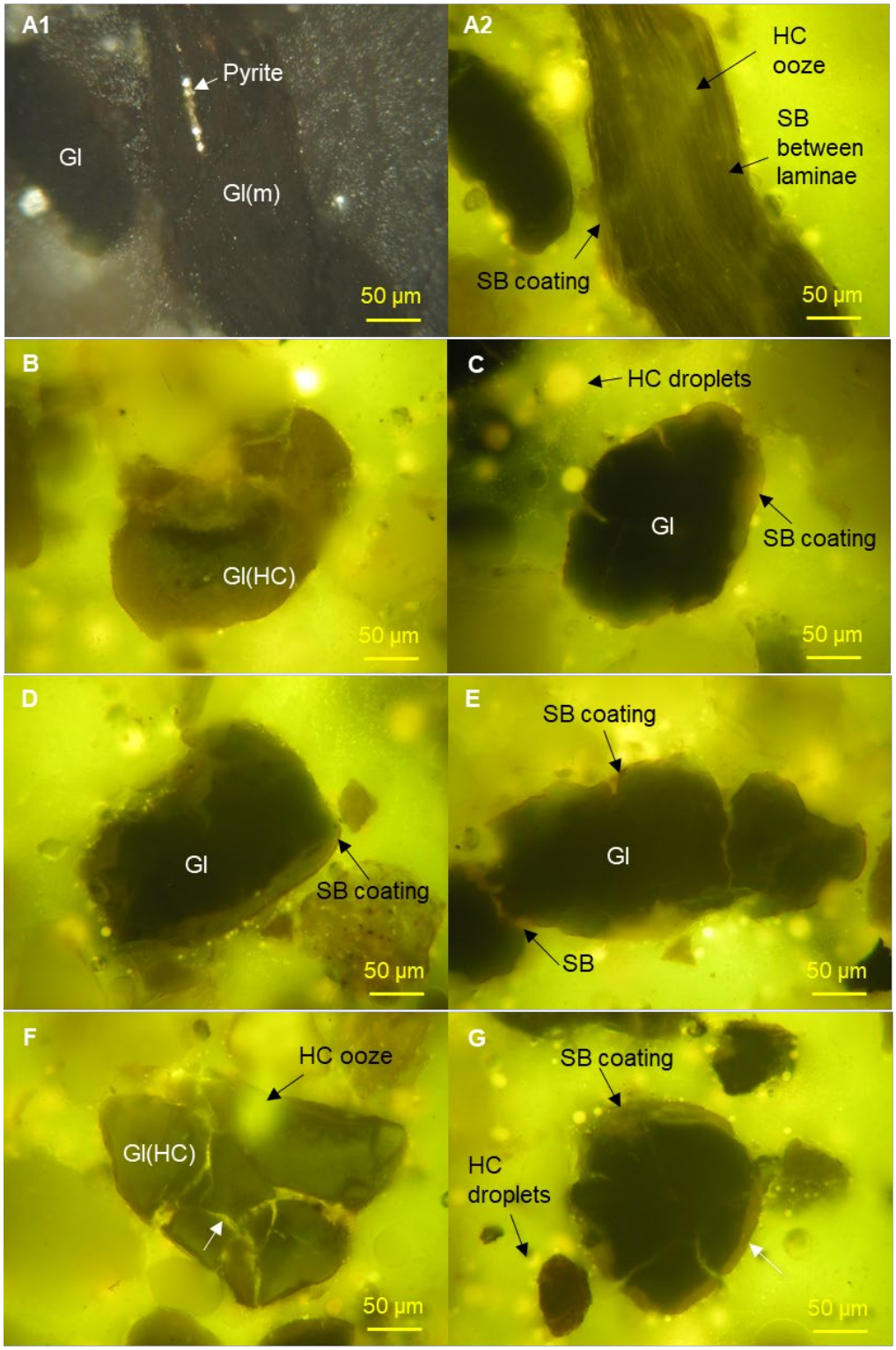

Figure 23. Photomicrographs in oil immersion of oil in the restored plug 94v-1. Yellowish fluorescing hydrocarbons are observed in the interior of the glauconite clasts (Gl[HC]), as droplets in the embedding resin, and as ooze. Orange-brownish fluorescing solid bitumen/asphaltenes (SB) occur as surface coating and in cracks of glauconite clasts. A1: reflected white light; A2–G: blue light illumination.

The oil occurs as coatings and in the interior of glauconite clasts, between the laminae of glauconised mica, and as a hydrocarbon ooze (Figure 23). Solid bitumen/asphaltenes amount to 5.88 vol.%, and the solid bitumen/asphaltene coatings are partly inherited from the hot Soxhlet extraction cleaned plug (0.67 vol.% in plug 94v-2; Table 4). In contrast, it is assumed that oil in the interior of the glauconite clasts was mainly introduced during the STO saturation and ageing process since the hot Soxhlet extraction cleaned plug did not show preserved remaining oil inside the glauconite clasts. The presence of mobile hydrocarbons is emphasised by yellowish fluorescing oil droplets in the embedding epoxy (Figure 23).

Concluding remarks

The restored plug is compositionally not fully comparable to the preserved core plugs. However, the preparation procedure largely replicates the hydrocarbon occurrences in the original plugs, including remaining oil coatings and oil in the interior of glauconite clasts. The estimated API of the prepared oil is like the measured range of crude oil APIs.

Supercritical CO_2-Flooded Restored Plug

The oil composition in the inlet samples from the scCO2-flooded restored plug 109 is significantly different from the pre-flooded restored plug (see composition of plug 94v-1; Table 4). The remaining oil volume and composition after scCO_2-flooding is very similar to the cleaned plugs (Table 4), testifying to a complete removal by scCO_2 of the mobile oil fractions leaving behind only the immovable solid bitumen/asphaltenes (Figure 24; Table 4). This is consistent with Jarboe et al. (2015), who demonstrated the ability of scCO_2 to mobilise remaining oil even in the high-mature Marcellus Shale, where aliphatic hydrocarbons in the range nC$_{11}$–nC$_{21}$ were dissolved, and Hwang and Ortiz (1998) who showed that CO_2 injection in the McElroy oil field caused significant deposition of heavy hydrocarbons >nC$_{25}$ in the reservoir near the injection well.

The solid bitumen/asphaltenes in the flooded plug occur as coatings, in the interior of glauconite clasts, and between the laminae of glauconised mica (Figure 25). Hydrocarbon ooze suggests that a minor fraction of lighter mobile oil remains (Figure 25). The coatings and the remaining oil in the interior of the glauconite clasts are mainly remnants after the scCO_2-flooding of the restored plug (see above). However, part of it represents a carry-over from the cleaned plug. This shows that similar to the various cleaning procedures, scCO_2 flooding cannot mobilise the solid bitumen/asphaltenes associated with glauconite, thus emphasising its stable condition in the reservoir matrix. In addition to the solid bitumen/asphaltenes, a small quantity of immobile oil was measured in the plug (Figure 24; Table 4). The recording of a fraction of immobile oil is consistent with the observation of an oil fraction not associated with glauconite (Figure 25). It is likely that this oil represents precipitated asphaltenes. Similarly, significant asphaltene precipitation was observed shortly after the start of CO_2 injection in the McElroy Field, resulting in about a 50% reduction of asphaltene content in the mobile oil (Hwang & Ortiz, 1998).

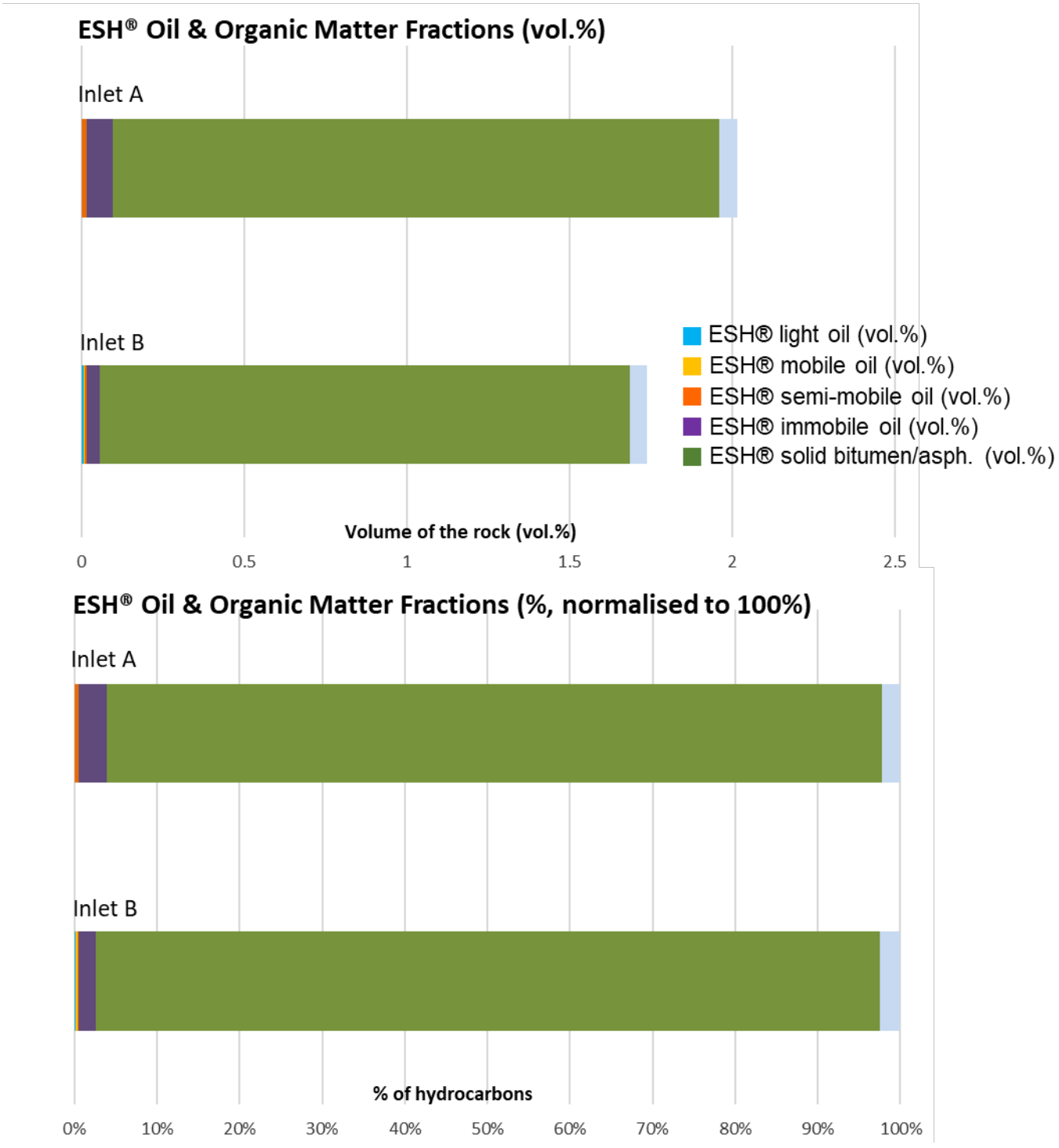

Figure 24. Histograms showing the composition of the remaining oil in the restored plug 94v-1 after flooding with $scCO_2$ under reservoir conditions. All mobile oil fractions have been extracted, while the remaining oil consists of solid bitumen/asphaltenes and a minor fraction of immobile oil. See also Table 4.

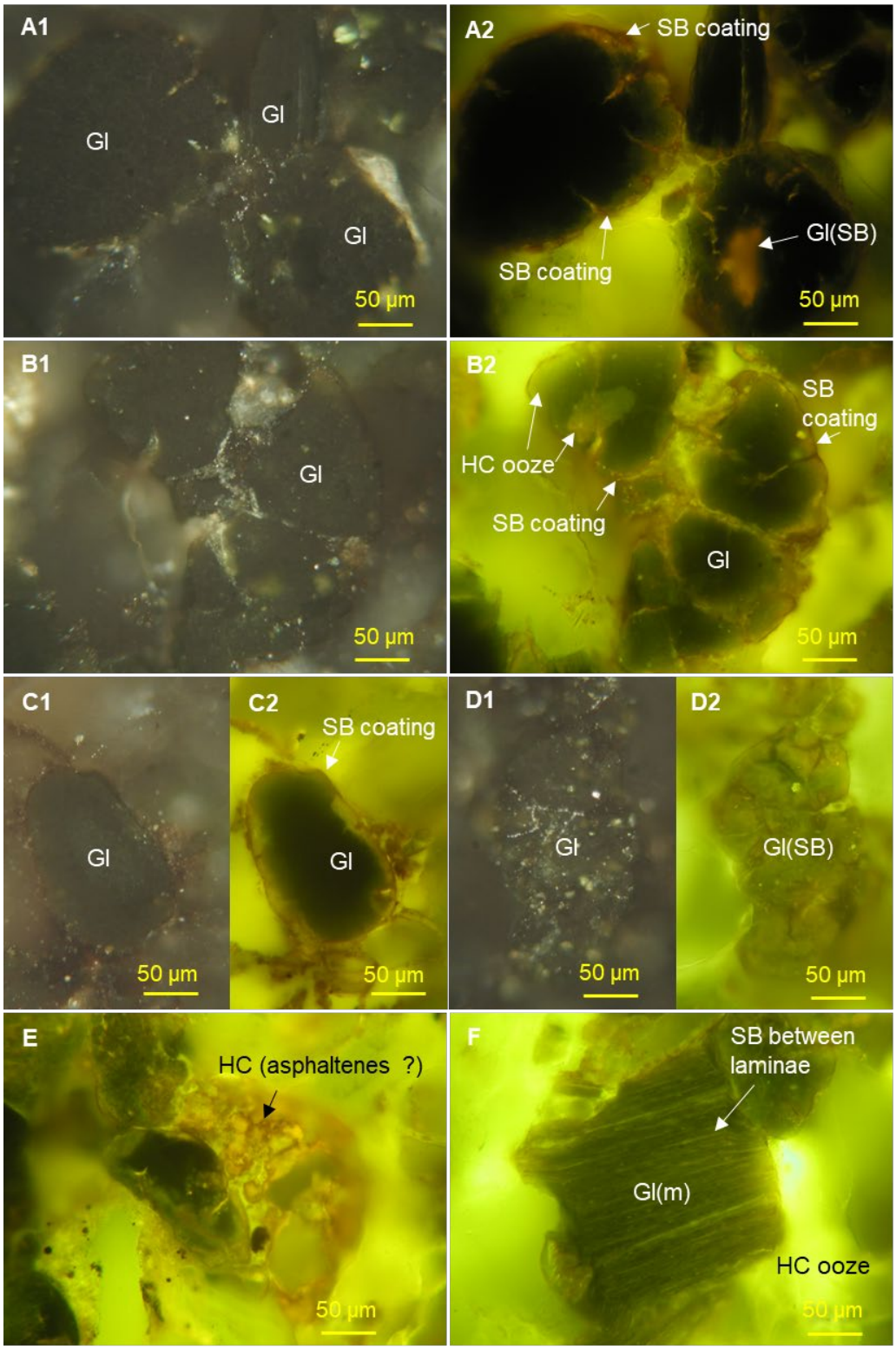

Figure 25. Photomicrographs in oil immersion of remaining oil in the $scCO_2$-flooded plug 109. Orange-brownish fluorescing solid bitumen/aspaltenes (SB) occur as surface coatings, in cracks, and in the interior of glauconite clasts (Gl[SB]), and between the laminae of glauconised mica (Gl[m]). Orange fluorescing hydrocarbons not associated with glauconite are possibly precipitated asphaltenes. A1–D1: reflected white light; A2–D2, E, F: blue light illumination.

Concluding Remarks

The hot soxhlet extraction cleaning method left behind a minor fraction of solid bitumen/asphaltenes (0.67 vol.% in plug 94v-2), and conversion of ESH data (vol.%) to saturation (%) shows that this proportion is only marginally higher in the restored $scCO_2$-flooded plug (see below). No substantial additional amounts of solid bitumen/asphaltenes are thus formed during $scCO_2$-flooding. The presence of solid bitumen/asphaltenes associated with glauconite not mobilised by $scCO_2$-flooding suggests it has a strong protective effect on the glauconite clasts, potentially preventing or at least limiting glauconite swelling and/or disintegration to fines. This is perhaps because the solid bitumen/asphaltenes coated glauconite surface is oil-wet. Likewise, glauconised mica with solid bitumen/asphaltenes between the laminae and glauconite clasts with solid bitumen/asphaltenes in the interior of the particle would – at least partly – be oil-wet. This could indicate mitigation of the formation and migration of glauconite fines which potentially can clog pore connectivity and thus deteriorate permeability (e.g. Pudlo et al., 2015; Wang et al., 2023). This does not exclude that glauconite clasts not associated with hydrocarbons could be water-wet and thus prone to swelling and fines formation.

Further, it is suggested that asphaltenes precipitated during $scCO_2$-flooding could harm $scCO_2$ injectivity by clogging pore throats in the reservoir. Hwang and Ortiz (1998) assumed that the recorded reduction in injectivity in the McElroy Field shortly after the start of CO_2 injection was caused by a reduction of porosity and effective permeability induced by the precipitation of heavy organic compounds. Asphaltenes are likely to be represented by the immobile oil fraction of which a minor quantity is recorded in plug 109 (Table 4). However, conversion of this proportion to saturation (%) reveal that the amount is inferior (see below), suggesting that asphaltene precipitation does not pose a risk to the $scCO_2$ injection.

Saturation Estimates and Porosity Correction

The results of the ESH show varying amounts of remaining hydrocarbons in the cleaned core plugs depending on the cleaning method (ranging from 0.67–1.76 vol.%). None of the cleaning methods resulted in complete removal of hydrocarbons. The porosity correction factor for each cleaned sample is calculated by applying the abovementioned procedure. The porosity underestimation ranges between (0.432 – 1.138 PU; see Table 5). However, the diffusion-evaporation method is considered unsuitable for cleaning the Nini-4 core plugs due to the presence of minor quantities of mobile and light hydrocarbons. The results from the cold flushed plug (96B) and the hot soxhlet extracted plug (91) are almost identical, suggesting that cold flushing is the best method to clean the core samples since applying the hot soxhlet extraction might compromise the integrity of the pore structure. In the case of plug 94v-2, the hot soxhlet extraction resulted in an impressive removal of the oil, in which only 1.29% (Table 6) of the pore volume was left uncleaned. This is equivalent to 0.432 PU porosity correction (Table 5), which is half the porosity underestimation compared to the other cleaning methods. This might be a result of the smaller dimensions relative to the rest of the core plugs. Plug 94v-2 has a length of 1.5 cm, equivalent to 15.62 cc, while the other plugs are from 5–7 cm, equivalent to 54.64–76.49 cc.

Table 5. Measured porosity, porosity correction factor (VHC/VT), and corrected porosity of the cleaned core samples.

Core Plug	Cleaning Method	$\phi_{measured}$	Oil	VHC/VT	$\phi_{corrected}$
		%	vol.%	%	%
96 (I)	Evaporation	35.39	1.76	1.138	36.53
96B	Cold flushed	35.46	1.29	0.834	36.30
91	Soxhlet	35.00	1.53	0.994	35.99
94v-2	Soxhlet	35.5	0.67	0.432	35.93

VHC: volume of hydrocarbons; VT: volume total

Table 6. ESH analysis results converted to saturations.

	Plug ID.	Total oil saturation (%)	Light oil saturation(%)	Mobile oil saturation (%)	Semimobile oil saturation (%)	Immobile oil saturation (%)	Solid bitumen saturation (%)
Preserved	93A	39.41	0.44	13.69	10.67	2.82	11.46
	$93F_2$	34.57	0.37	13.64	9.27	2.11	8.85
	X	48.45	0.50	13.92	19.68	5.16	9.06
	89A	22.74	0.14	7.68	5.80	1.33	7.47
	98B	38.11	0.45	11.15	12.61	4.69	9.03
	114A	17.88	0.04	3.36	4.00	1.22	8.91
Cleaned	96 (I)	3.33	0	0.21	0.16	0	2.75
	96B	2.50	0	0	0	0	2.30
	91	2.94	0	0	0	0	2.76
	94v-2	1.29	0	0	0	0	1.20
Restored	94v-1	70.69	1.29	22.91	24.93	6.37	14.65
$scCO_2$ flooded	109	3.67	0	0	0.02	0.15	3.39
	109	3.15	0	0	0	0.07	2.96

A small piece of sample material was collected from plug 94v-2 for ESH analysis, while the rest of the core plug went through the restoration process and was tagged as plug 94v-1. During this process, the core was placed under a vacuum for two hours and brine was introduced to the system to ensure complete saturation of the pore space with brine. This was confirmed by the Archimedes method, in which the core is submerged in a pool of brine, and the buoyancy force was measured. The sample was then drained to the connate water saturation (S_{wi}=30%) using the porose plate method, where the plug was placed in a core holder equipped with a semi-permeable ceramic plat that only allowed the flow of brine out of the core and retained the flow of gas. The N_2 gas was then replaced with STO under vacuum, after which the plug underwent the ageing procedure. This way, the exact fluid (brine and oil) saturations were ensured (S_w=30% and S_o=70%). Knowing the appropriate porosity correction and the exact saturations, plug 94v-1 was used to validate the ESH method and estimate the accuracy of the saturations calculated from the ESH results. The resulting saturation for plug 94v-1 is 70.69% in the case of including the matrix-associated solid hydrocarbons and 70.16% if the associated solid hydrocarbons are excluded, which is almost the exact measured saturation value of 70%. An average porosity correction factor of 0.8 PU was applied for the preserved plugs and the

$scCO_2$-flooded plug 109 (no ESH data on the cleaned plugs for these specific samples) before converting the ESH vol.% to oil saturations (Table 6).

Comparing the oil saturations of fresh state and brine stored plugs, most of the mobile oil saturation and a significant fraction of the semi-mobile oil have been expelled by gravity from the core plugs stored in brine. In contrast, no change in the immobile oil and solid bitumen/asphaltenes saturations are observed. In the case of core plug 98B, an anomaly can be observed in the data where no oil mobilisation occurred under brine gravity. This could result from a lack of brine coverage, or the analysed sample piece was taken from the topmost part of the sample where gravity forces are minimal.

The results on the restored plug 94v-1 show higher saturation of immobile oil and solid bitumen/asphaltenes compared to the preserved sample, opposite to the expectation. This difference is explained by the ageing process, during which a layer of heavy oil adheres to the surface of the (glauconite) grains, which causes a wettability alteration; flushing the sample with fresh STO is believed to leave this fraction on the grains resulting in a higher heavy oil fraction. The results from the $scCO_2$-flooded plug 109 reveals that negligible amounts of light, mobile, semi-mobile, and immobile oil are left behind (Table 4). Further, comparison of the solid bitumen/asphaltenes saturation of plug 109 with the solid bitumen/asphaltenes saturations of the cleaned core plugs shows similar saturations, which together with the inferior immobile oil fraction after $scCO_2$-flooding indicate no or very low risk of asphaltene precipitation.

The light and mobile oil saturations of the preserved plugs and the restored plug were lumped into the group “movable oil saturation” (Table 7). Similarly, the immobile and solid bitumen/asphaltenes saturations were lumped into “non-movable oil saturation” group (Table 7). The semi-mobile oil fraction was kept as it is since its mobile and immobile oil fractions are not known. The total oil saturation and the combined constituents of movable, semi-movable and non-movable oil saturations in the preserved core plugs and the restored 94v-1 plug are shown in Table 7.

It is notable that the non-movable oil saturations of the preserved core plugs are within the range of residual oil saturation, S_{or}, of 8–15% reported in the conventional core analysis (CCAL) report (MacDonald and Mair, 2003). Like the preserved plugs, the non-movable oil saturation of the restored core plug 94v-1 is similar to the residual oil saturation of S_{or}=19.74% in plug 109 (also restored) after water flooding. This indicates that the ESH method might be used as a quick estimate of the residual oil saturation after water flooding. However, this needs further investigation since no ESH analysis has been conducted on a water flooded sample, thus further investigation is needed to validate this assumption.

Table 7 Lumped saturation of the preserved and the restored samples.

	Plug ID.	Total oil saturation (%)	Movable oil saturation(%)	Semi-movable oil saturation (%)	Non-movable oil saturation (%)
Preserved	93A	39.41	14.13	10.67	14.28
	$93F_2$	34.57	14.01	9.27	10.96
	X	48.45	14.42	19.68	14.22
	89A	22.74	7.82	5.80	8.80
	98B	38.11	11.60	12.61	13.72
	114A	17.88	3.40	4.00	10.13
Restored	94v-1	70.69	24.20	24.93	21.03

MAIN FINDINGS

The main findings of the study of the remaining oil are:

1. The STO oil contains a minor amount of asphaltenes and shows only limited OBM contamination in the diesel range. OBM contamination will thus not interfere with the heavy oil fraction >nC_{20} that potentially may pose problems with clogging.

2. The remaining oil in the preserved plugs consists of c. 11–15 vol.% (56–65% normalised) mobile oil and c. 5–7 vol% (35–44% normalised) immobile oil and solid bitumen/asphaltenes. The cleaning procedures remove the mobile and immobile oil fractions, but none of the cleaning methods removes all the solid bitumen/asphaltenes associated with glauconite. The solid bitumen/asphaltenes occur in the interior of glauconite clasts, as coatings on the surface, and in small cracks in the surface, as well as between the laminae of glauconised mica. Of the three cleaning methods, hot Soxhlet extraction was the most efficient, but still, minor remains of solid bitumen/asphaltenes are visible as surface coatings and in small cracks in the surface of the glauconite clasts. This remaining solid bitumen/asphaltenes are 'carried' over to the restored (STO saturated and aged) plugs used for scCO_2-flooding experiments.

3. A hot Soxhlet extraction cleaned plug was restored with STO and aged for one month. Remaining oil is seen as surface coatings and in the interior of glauconite clasts, between the laminae of glauconised mica, and as a hydrocarbon ooze. The oil coatings were partly inherited from the cleaned plug, while the oil in the interior of the glauconite clasts was mainly introduced during the preparation process. The restored oil composition is, overall, comparable to the composition of the oil in the preserved plugs.

4. Supercritical CO_2-flooding of a restored plug shows that the mobile oil fractions are removed while the solid bitumen/asphaltene coatings and remnants in the interior of the glauconite clasts were not mobilised, suggesting:

- The solid bitumen/asphaltenes are immobile and non-reactive, and glauconite clasts with a solid bitumen/asphaltenes surface coating can be considered to have oil-wet surfaces. The same applies to areas inside the glauconite clasts containing solid bitumen/asphaltenes and glauconised mica with solid bitumen/asphaltenes between the laminae. The solid bitumen/asphaltenes may thus have a protective effect, potentially mitigating glauconite swelling, disintegration, and fines generation. Glauconite not associated with solid bitumen/asphaltenes is likely water-wet and prone to both swelling and disintegration into fines.

5. Negligible amounts of immobile oil is left behind in the scCO_2-flooded plug 109. Further, the solid bitumen/asphaltenes saturations of plug 109 and the cleaned core plugs are very similar, which together with the inferior immobile oil fraction indicate:

- No or very low risk of asphaltene precipitation.

6. Measured He-porosity is slightly underestimated due to the presence of non-mobile solid bitumen/asphaltenes. ESH analyses on cleaned samples provide the amount of solid bitumen/asphaltenes which cannot be removed by cleaning. A method to convert the results of vol.%-ESH to %-saturation has been derived, and the equation required to correct the He-porosimeter porosity measurements by a correction factor has been developed based on the results of the ESH from cleaned core plugs. The porosity underestimation ranges from 0.432–1.138 PU.

7. Knowing the appropriate porosity correction and the exact saturations, plug 94v-1 was used to validate the ESH method and estimate the accuracy of the saturations calculated from the ESH results. The resulting total oil saturation for plug 94v-1 is 70.69% in the case of including the matrix-associated solid hydrocarbons and 70.16% if the associated solid hydrocarbons are excluded, which is almost the exact measured oil saturation of 70%.

8. The non-movable oil saturations derived from ESH of the preserved core plugs are within the range of residual oil saturations (S_{or}=8–15%) determined by conventional core analysis. Further, the non-movable oil saturation of the restored core plug 94v-1 (21.03%) is close to the residual oil saturation of S_{or}=19.74% in the restored plug 109 after water flooding:

- This indicates that the ESH method might be used to provide a fast and low-cost estimate of the residual oil saturation after water flooding. This assumption should be verified by ESH analysis of water flooded samples.

ACKNOWLEDGMENT

This study is part of Project Greensand Phase 2, aiming to store CO_2 in the depleted Nini West oil field in the Siri Canyon, Danish North Sea. The Greensand Phase 2 Consortium consists of 23 Danish and international industrial and academic partners. The project is funded by the Danish Energy Technology Development and Demonstration Program (EUDP grant #64021-9005).

REFERENCES

Alpern, B., Lemos de Sousa, M.J., Pinheiro, H.J., Zhu, X., 1992. Optical morphology of hydrocarbons and oil progenitors in sedimentary rocks – relations with geochemical parameters. Publ. Museu. Lab. Miner. Geol. Fac. Ciên Porto Nova Série 3, 53 pp.

Danish Energy Agency, 2014. Oil and gas production in Denmark in 2013. The Danish Energy Agency, 105 pp.

Dong E&P, 2003. Final well report. License 4/95 Nini-4/4A, 187 pp.

Geochemical Investigations Ltd., 2003. A show detection, characterization and correlation study involving samples from the Nini-4 (5605/10-4) well and Nini-4A (5605/10-4A) sidetrack, offshore Denmark, and comparison with previously analysed fluids and shows. Report 02/12942/03/01, 227 pp.

Goodarzi, F., Gentzis, T., Grasby, S.E. and Dewing, K., 2018. Influence of igneous intrusions on thermal maturity and optical texture: comparison between a bituminous marl and a coal seam of the same maturity. Int. J. Coal Geol. 198, 183–197.

Hagemann, H.W. and Hollerbach, A., 1986. The fluorescence behaviour of crude oils with respect to their thermal maturaty and degradation. Org. Geochem. 10, 473–480.

Hamberg, L., Dam, G., Wilhelmson, C. and Ottesen, T.G., 2005. Paleocene deep-marine sandstone plays in the Siri Canyon offshore Denmark-southern Norway. In: Doré, A. G. and Vining, B.A. (Eds.), Petroleum geology: North-West Europe and global perspectives. Proceedings of the 6th Petroleum Geology Conference. London. Geol. Soc., pp. 1185–1198

Hunt, J.M., 1996. Petroleum geochemistry and geology. W.H. Freeman and Company, New York, second edition, 743 pp.

Hwang, R.J. and Ortiz, J., 1998. Effect of CO_2 flood on geochemistry of the McElroy oil. Org. Geochem. 29, 485–503.

Jacob, H., 1989. Classification, structure, genesis and practical importance of natural solid oil bitumen ("migrabitumen"). Int. J. Coal Geol. 11, 65–79.

Jarboe, P.J., Candela, P.A., Zhu, W. and Kaufman, A.J., 2015. Extraction of hydrocarbons from high-maturity Marcellus Shale using supercritical carbon dioxide. Energy Fuels 29, 7897–7909.

Keulen, N., Weibel, R. and Malkki, S.N., 2022. Mineral-specific quantitative element mapping applied to visualization of the geochemical variation in glauconite clasts. Frontiers Earth Sci. 10:788781; doi:10.3389/feart.2022.788781.

Kus, J., Khanaqa, P., Mohialdeen, I.M.J., Kaufhold, S., Babies, H.G., Messner, J. and Blumenberg, M., 2016. Solid bitumen, bituminite and thermal maturity of the Upper Jurassic–Lower Cretaceous Chia Gara Formation, Kirkuk Oil Field, Zagros Fold Belt, Kurdistan, Iraq. Int. J. Coal Geol. 165, 28–48.

Landis, C.R. and Castaño, J.R., 1995. Maturation and bulk chemical properties of a suite of solid hydrocarbons. Org. Geochem. 22, 137–149.

MacDonald, I. and Mair, K., 2003. Conventional core analysis report. Nini-4 well. Robertson Research International Limited, Report number AF790.

Mastalerz, M., Drobniak, A., Stankiewicz, A.B., 2018. Origin, properties, and implications of solid bitumen in source-rock reservoirs: a review. Int. J. Coal Geol. 195, 14–36.

Nielsen, O.B., Rasmussen, E.R. and Thyberg, B.I., 2015. Distribution of clay minerals in the northern North Sea basin during the Paleogene and Neogene: A result of source-area geology and sorting processes. J. Sedim. Res. 85, 562–581.

Petersen, H.I., 2017. Source rock, types and petroleum generation. Chapter 4. In: Suárez-Ruiz, I. and Filho, J.G.M. (Eds.), Geology: current and future developments vol. 1, Bentham Science Publishers, 105–131.

Petersen, H.I., Springer, N., Weibel, R. and Schovsbo, N.H., 2022. Sealing capability of the Eocene–Miocene Horda and Lark formations of the Nini West depleted oil field – implications for safe CO_2 storage in the North Sea. Int. Journ. Greenh. Gas Contr. 118; doi.org/10.1016/j.ijggc.2022.103675

Pickel, W., Kus, J., Flores, D., Kalaitzidis, S., Christanis, K., Cardott, B.J., Misz-Kennan, M., Rodrigues, S., Hentschel, A., Hamor-Vido, M., Crosdale, P., Wagner, N., ICCP, 2017. Classification of liptinite - ICCP System 1994. Int. J. Coal Geol. 169, 40–61.

Pradier, B., Largeau, C., Derenne, S., Martinez, L., Bertrand, P. and Pouet, Y., 1990. Chemical basis of fluorescence alteration of crude oils and kerogens – I. Microfluorimetry of an oil and its isolated fractions; relationships with chemical structure. Org. Geochem. 16, 451–460.

Pudlo, D., Henkel, S., Reitenbach, V., Albrecht, D., Enzmann, F., Heister, K., Pronk, G., Ganzer, L. and Gaupp, R., 2015. The chemical dissolution and physical migration of minerals induced during CO_2 laboratory experiments: their relevance for reservoir quality. Environ. Earth Sci. 73, 7029–7042.

Radke, M., Willsch, H. and Welte, D.H., 1980. Preparative hydrocarbon group determination by automated medium pressure liquid chromatography. Anal. Chem. 52, 406–411.

Sanei, H., 2020. Genesis of solid bitumen. Sci. Reports 10:15595; doi.org/10.1038/s41598-020-72692-2.

Schiøler, P., Andsbjerg, J., Clausen, O.R., Dam, G., Dybkjær, K., Hamberg, L., Heilman- Clausen, C., Johannessen, E.P., Kristensen, L.E., Prince, I. and Rasmussen, J.A., 2007. Lithostratigraphy of the Palaeogene – Lower Neogene succession of the Danish North Sea. Geol. Surv. Denm. Greenl. Bull. 12, 77 pp.

Schovsbo, N.H., Petersen, H.I., Weibel, R., Holmslykke, H.D. and Springer, N., 2021. Characterising and evaluation of the seal capacity based on core and cutting analysis of the Nini-4 and Nini-4a wells. Project Greensand – WP4 final report. Danm. Grønl. Geol. Unders. Rapport 2021/38.

Slaattedal, H.O., 2022. Geochemistry data report – SARA analysis of one oil sample. Applied Technology Norway A/S, APT22-6732, 4 pp.

Stasiuk, L.D. and Snowdon, L.R., 1997. Fluorescence micro-spectrometry of synthetic and natural hydrocarbon fluid inclusions: crude oil chemistry, density and application to petroleum migration. Appl. Geochem. 12, 229–241.

Svendsen, J., Hansen, H., Stærmose, T. and Engkilde, M., 2010. Sand remobilization and injection above an active salt diapir: the Tyr Sand of the Nini Field. Eastern North Sea. Basin Res. 22, 548–561.

Teichmüller, M., 1974. Über neue Macerale der Liptinit-Gruppe und die Entstehung von Micrinit. Fortschr. Geol. Rheinld. Westf. 24, 37–64.

Tissot, B.P. and Welte, D.H., 1984. Petroleum formation and occurrence. Springer-Verlag, Berlin Heidelberg, second revised and enlarged edition, 699 pp.

Wang, K., Ma, L. and Taylor, K.G., 2023. Microstructure changes as a response to CO_2 storage in sedimentary rocks: recent developments and future challenges. Fuel 333; doi.org/10.1016/j.fuel.2022.126403.

Weibel, R., Friis, H., Kazerouni, A.M., Svendsen, J.B., Stokkendal, J. and Poulsen, M.L.K., 2010. Development of early diagenetic silica and quartz morphologies – examples from the Siri Canyon. Danish North Sea. Sed. Geol. 228, 151–170.

Weibel, R., Keulen, N., Olivarius, M., Malkki, S.N., Holmslykke, H.D., Mohammadkhani, S., Olsen, D. and Schovsbo, N.H., 2021. Petrography and mineralogy of greensand in the Nini area including mineral reactions in CO_2 flooding experiments. Danm. Grønl. Geol. Unders. Rapport 2021/40.

Årland, K.S. and Bastow, M., 2016. Quantifying mud contamination without adding tracers. Int. Symp. Soc. Core Analysis, SCA2016-32, 12 pp.